HOXA1 binds RBCK1/HOIL-1 and TRAF2 and modulates the TNF/NF-κB pathway in a transcription-independent manner.

Taminiau, Arnaud; Draime, Amandine; Tys, Janne; Lambert, Barbara; Vandeputte, Julie; Nguyen, Nathan; Renard, Patricia; Geerts, Dirk; Rezsohazy, René

Published in:
Nucleic Acids Research

DOI:
10.1093/nar/gkw606

Publication date:
2016

Document Version
Publisher's PDF, also known as Version of record

Published online 5 July 2016

Nucleic Acids Research, 2016, Vol. 44, No. 15 ***7331–7349***
doi: 10.1093/nar/gkw606

HOXA1 binds RBCK1/HOIL-1 and TRAF2 and modulates the TNF/NF-κB pathway in a transcription-independent manner

Arnaud Taminiau[1], Amandine Draime[1], Janne Tys[1], Barbara Lambert[1], Julie Vandeputte[1], Nathan Nguyen[1], Patricia Renard[2], Dirk Geerts[3] and René Rezsöhazy[1,*]

[1]Animal Molecular and Cellular Biology Group (AMCB), Life Sciences Institute (ISV), Université catholique de Louvain, Louvain-la-Neuve 1348, Belgium, [2]Cellular Biology Research Unit, Université de Namur, Namur 5000, Belgium and [3]Department of Pediatric Oncology/Hematology, Erasmus University Medical Center, Rotterdam 3015, The Netherlands

Received November 26, 2015; Revised June 22, 2016; Accepted June 24, 2016

ABSTRACT

HOX proteins define a family of key transcription factors regulating animal embryogenesis. *HOX* genes have also been linked to oncogenesis and *HOXA1* has been described to be active in several cancers, including breast cancer. Through a proteome-wide interaction screening, we previously identified the TNFR-associated proteins RBCK1/HOIL-1 and TRAF2 as HOXA1 interactors suggesting that HOXA1 is functionally linked to the TNF/NF-κB signaling pathway. Here, we reveal a strong positive correlation between expression of *HOXA1* and of members of the TNF/NF-κB pathway in breast tumor datasets. Functionally, we demonstrate that HOXA1 can activate NF-κB and operates upstream of the NF-κB inhibitor IκB. Consistently, we next demonstrate that the HOXA1-mediated activation of NF-κB is non-transcriptional and that RBCK1 and TRAF2 influences on NF-κB are epistatic to HOXA1. We also identify an 11 Histidine repeat and the homeodomain of HOXA1 to be required both for RBCK1 and TRAF2 interaction and NF-κB stimulation. Finally, we highlight that activation of NF-κB is crucial for HOXA1 oncogenic activity.

INTRODUCTION

HOX proteins constitute an evolutionary conserved family of transcription factors critically involved in regulating biological processes during embryogenesis from patterning the main body axis to coordinating organogenesis and differentiation in all bilaterian animals (1). Mammalian genomes contain 39 *HOX* genes which are clustered in four chromosomal loci and classified in 13 paralog groups with respect to their sequence similarity, their arrangement along the chromosomes and the timing of their expression during development (2,3).

HOXA1 is the first *HOX* gene to be expressed in connection with gastrulation during embryogenesis. It is primarily involved in hindbrain segmentation into rhombomeres. Next, *HOXA1* is required to determine the identity of rhombomeres r4 and r5, and to specify the associated neural crest. It also contributes to inner and middle ear development, basioccipital bone formation and patterning of the great arteries and outflow tract of the heart (4–6). Over the last two decades, *HOXA1* has been linked to adult cancers in breast, lung, liver, prostate and the oral cavity, as well as to melanoma (7–12). In the context of breast cancer, *HOXA1* has been identified as a mammary epithelial oncogene, where its forced expression is sufficient to induce the oncogenic transformation of immortalized human mammary epithelial cells to aggressive *in vivo* carcinoma (11,13).

While the functions and to some extent target genes of HOXA1 have been well documented, the molecular modalities of HOXA1 activities remain scarcely characterized. So far, two functional domains of the HOXA1 protein have been clearly identified. The 60 amino acids long homeodomain shared by all HOX proteins defines their DNA-binding domain which folds into three α-helices preceded by a flexible N-terminal extension. The third helix and the N-terminal extension are involved in specific contacts with DNA (1,14). The so-called hexapeptide lies N-terminally to the homeodomain extension. It is a six amino-acid long motif conserved in HOX proteins from paralog groups 1 to 9 involved in the interaction with PBX proteins, the best characterized HOX interactors which belong to the 'Three Amino acid Loop Extension' (TALE) class of homeodomain transcription factors. The integrity of the hexapeptide and the interaction with PBX is crucial for HOXA1 transcriptional activity in several reported cases. In fact, hexapeptide mutations disrupting the HOXA1–PBX interaction lead to a

*To whom correspondence should be addressed. Tel: +32 10 47 37 01; Fax: +32 10 47 37 17; Email: rene.rezsohazy@uclouvain.be

phenocopy of the HOXA1 knockout in the mouse (15) as well as to a loss of its oncogenic potential (16). In addition to these well-characterized functional determinants, the N-terminal moiety of human HOXA1 contains two histidine (His) repeats of ten and five residues, respectively. These repeats are conserved among HOXA1 orthologs, although the size of the longest His repeat varies, the mouse protein containing 11 and 5 His tracts, respectively. The function of these His repeats remains unexplored, but His repeat length variations have been reported in cases of autism in the Japanese population and *in vitro* expression of expanded His-repeat variants of HOXA1 resulted in a loss of cooperative binding with PBX1, leading to nuclear protein aggregation, impaired neuronal differentiation and cell death (17–19). His deletion within the HOXA1 sequence has also been found in ventricular septal defect patients (20). Together, these results suggest that these His repeats critically influence the function of the HOXA1 protein.

Protein–protein interactions mechanistically support the function of regulatory proteins like transcription factors or signal transducers. For the HOX family, the large repertoires of proteins HOX transcription factors are expected to interact with still need to be identified. Only two extensive searches for HOX interactors have been previously performed focusing on UBX in Drosophila (21) and HOXA1 in mammals (22). From the proteome-wide yeast two hybrid screening we recently carried out to pinpoint HOXA1 protein partners, 41 candidate interactors were confirmed by both affinity co-precipitation and Bimolecular Fluorescence Complementation assays. Most significantly, the validated HOXA1 interactors comprised proteins known to be active in transcription regulation, but also proteins involved in cell signaling like in focal adhesion, receptor tyrosine kinase function, and the TGFβ/BMP and Tumor Necrosis Factor (TNF)/Nuclear Factor kappa B (NF-κB) pathways (22).

The HOXA1 interactor proteins we identified as part of the Tumor Necrosis Factor Receptor (TNFR) family included RBCK1 (NCBI GeneID 10616, also known as HOIL-1) and TRAF2 (NCBI geneID 7186). TNF signaling is crucial for physiological processes like cell proliferation, differentiation, apoptosis, immune response modulation and inflammation induction. Binding of the pro-inflammatory cytokine TNFα to TNFR initiates a signaling cascade starting with the recruitment of TRADD (TNF receptor-associated death domain) that further recruits other proteins: cIAP1 and cIAP2 (cellular inhibitor of apoptosis 1 and 2), RIPK1 (receptor-interacting protein kinase 1), TRAF2 and TRAF5 (TNF receptor-associated factors 2 and 5). RIPK1 is then poly-ubiquitinated allowing docking of TAK1 (transforming growth factor-β-activated kinase 1) in complex with TAB2 and TAB3 (TAK1 binding protein 2 and 3), and the IKK (Inhibitor of NF-κB kinase) complex subunits IKKα, IKKβ and NEMO. The formation of the IKK complex can be enhanced by the presence of the LUBAC complex, constituted of three proteins: RBCK1 (HOIL-1), SHARPIN and HOIP (23–25). Oppositely, RBCK1 has also been suggested to display an inhibitory influence toward NF-κB by negatively regulating TAB2/TAB3 and targeting them for proteasomal degradation, thereby impairing NF-κB activation (26). Downstream of the IKK complex are the NF-κB transcription factors (p65/RelA, RelB, c-Rel, p50/NF-κB1 and p52/NF-κB2) that can form different heterodimers, the most common being the p65/p50 heterodimer (27). Under basal conditions, NF-κB is held inactive in the cytoplasm by IκB proteins (28). Upon activation of the pathway, the phosphorylation of IKKα and IKKβ by TAK1 acts as a switch; activating NF-κB by targeting IκB for phosphorylation, poly-ubiquitination and subsequent proteasome-dependent degradation, allowing NF-κB release and nuclear translocation to engage transcriptional programs (29–31).

Since NF-κB regulates more than 500 genes involved in inflammation, cellular transformation, survival, proliferation, angiogenesis, invasion and metastasis (32,33), aberrant NF-κB activation is frequently observed in adult cancers in breast, lung, liver and the oral cavity, and in melanoma (31,34,35), just like HOXA1 (7–11). Genetic alterations in multiple actors of the NF-κB pathway have been shown to be essential for cancer initiation. The E3 ubiquitin ligase RBCK1 has for example been reported as implicated in breast cancer where it stimulates proliferation by promoting the cell cycle (36) and TRAF2 is an oncogene that is amplified in 15% of human epithelial cancers (37). Therefore, the NF-κB pathway and HOXA1 expression could be functionally connected in the context of defined cancers.

The validation of the direct interaction between HOXA1 and RBCK1 and TRAF2 led us to hypothesize that HOXA1 can functionally connect to TNFR-signaling at the protein-binding level, and thereby directly modulate TNFR stimulation output. To possibly link this interaction to tumorigenic processes and to highlight to what extent HOXA1 expression could be correlated to the NF-κB signaling pathway, we analyzed public breast cancer datasets. Next, we investigated whether HOXA1 could influence the TNFR-mediated NF-κB activation. In the present study we first establish a highly significant positive correlation between expression of HOXA1 and of members of the TNF/NF-κB signaling pathway in breast tumors. Then, we demonstrate (i) that HOXA1 can activate NF-κB both independently and in synergy with TNFα stimulation, in a specific and non-transcriptional fashion, (ii) that HOXA1 operates upstream of the NF-κB inhibitor IκB and triggers IKKα/β and p65 phosphorylation as well as p65 nuclear translocation, (iii) that the RBCK1 and TRAF2 influences on the NF-κB response are epistatic to HOXA1, (iv) that removal of the HOXA1 His repeat or homeodomain diminishes both its interactions with RBCK1 and TRAF2 and its capacity to stimulate the TNF/NF-κB pathway and (v) that activation of NF-κB is crucial for HOXA1 oncogenic activity.

MATERIALS AND METHODS

Analysis of public breast cancer expression profiling datasets

All genome-wide expression profiling datasets of breast cancer patients with a sample size >80 available in the public domain ($n = 20$) were retrieved from the public Gene Expression Omnibus (GEO) dataset on the NCBI website (http://www.ncbi.nlm.nih.gov/geo/), and analyzed using R2: a genomics analysis and visualization platform de-

veloped in the Department of Oncogenomics at the Academic Medical Center—University of Amsterdam (http://r2.amc.nl). The Chin-124 set was uploaded from EMBL EBI (http://www.ebi.ac.uk/arrayexpress) under E-TABM-158. Expression data (CEL files) were analyzed as described previously (38). Briefly, gene transcript levels were determined from data image files using GeneChip operating software (MAS5.0 and GCOS1.0, from Affymetrix). Samples were scaled by setting the average intensity of the middle 96% of all probe-set signals to a fixed value of 100 for every sample in the dataset, allowing comparisons between micro-arrays. Five datasets that showed no HOXA1 mRNA expression (GSE1456, -3494, -5462 and -12 093), or did not yield HOXA1-correlating genes (GSE50948) were excluded from further analysis.

The TranscriptView genomic analysis and visualization tool within R2 was used to check if probe-sets had an anti-sense position in an exon of the gene (http://r2.amc.nl > genome browser). The probe-sets selected for HOXA1 (Affymetrix 214639_s_at and Illumina 1700382) and for all KEGG NF-κB pathway genes (Supplementary Table S1) meet these criteria. All expression values and other details for the datasets used can be obtained through their GSE or E number from the NCBI GEO and EBI ArrayExpress websites, respectively.

Cell culture, transfection and treatment

MCF10A cells were maintained in Dulbecco's modified Eagle medium (DMEM) F12 (Invitrogen, Carlsbad, California, USA) supplemented with 5% Horse Serum (Invitrogen), 100 IU/ml penicillin and 100 μg/ml streptomycin (Sigma-Aldrich, Saint-Louis, Missouri, USA), 0.1 μg/ml cholera toxin (Sigma-Aldrich), 10 μg/ml insulin (Sigma-Aldrich), 0.5 μg/ml hydrocortisone (Sigma-Aldrich) and 20 ng/ml human epidermal growth factor (Invitrogen). MCF7 cells were maintained in DMEM 4.5 g/l D-glucose supplemented with 10% fetal bovine serum (Invitrogen), 100 IU/ml penicillin and 100 μg/ml streptomycin, 2 mM L-glutamine (Invitrogen) and 1 mM sodium pyruvate. COS7 and HEK293T cells were maintained in DMEM low or high glucose, respectively (Invitrogen) supplemented with Glutamine, 10% fetal bovine serum (Invitrogen), 100 IU/ml penicillin and 100 μg/ml streptomycin (Sigma-Aldrich). All cells were maintained at 37°C in a humidified 5% CO_2 atmosphere.

MCF10A cells were transfected with X-treme Gene 9 DNA Transfection Reagent (Roche, Indianapolis, IN, USA). MCF7, HEK293T and COS7 cells were transfected with jetPRIME Transfection Reagent (Polyplus Transfection, Illkirch, France). All transfections were performed 24 h after plating and were carried out following the manufacturer's instructions.

Where stated, Tumor Necrosis Factor α (TNFα) or Interleukin-1-beta (IL-1β) (both from Sigma-Aldrich) were added to the medium (25 ng/ml final concentration) 24 h post-transfection for the indicated time.

Plasmids

Reporter plasmid pGL4.32[luc2P/NF-κB-RE/Hygro] (Promega, Madison, Wisconsin, USA) contains the luciferase reporter gene luc2P controlled by five copies of a 10-nt NF-κB responsive element corresponding to p65 binding sites (39). Reporter plasmids pML-EPHA2-r4-Luc (40) and pCMV-LacZ (41), expression plasmids for $HOXA1^{WT}$ (pGIH-309), $HOXA1^{QN\text{-}AA}$ (pGIH-512), $HOXA1^{WM\text{-}AA}$ (pGIH-328) Flag-HOXA2 (42) and PBX1 (pCMV-PBX1) (43), the expression plasmid for PREP1 (44), the pEXP-FLAG(Nter)-HOXA1, pEXP-VC155(Nter)-HOXA1, pEXP-VN173(Nter)-HOXA1, pEXP-GST(Nter)-RBCK1, pEXP-VN173(Nter)-RBCK1, pEXP-GST(Nter)-TRAF2 and pEXP-VN173(Nter)-TRAF2 vectors (22) and HOXA1 mutants generated by pentapeptide insertion mutagenesis (45) were all described previously. The HOXA1 deletion derivatives $HOXA1^{\Delta Nter}$, $HOXA1^{\Delta 11His}$, $HOXA1^{\Delta 77\text{-}205}$, $HOXA1^{\Delta HD}$ and $HOXA1^{\Delta Cter}$ were generated by overlapping polymerase chain reaction using the primers listed in Supplementary Table S2 and swapping in pEXP expression vectors for HOXA1 using the Gateway® system (Life Technologies, Carlsbad, California, USA) following manufacturers's instructions. All HOXA1 constructs were based on the canonical 336 amino acid isoform (RefSeq NP_034579). Expression plasmids for HOXA9, HOXB9 and HOXD9 were kind gifts from Dr Deneen Wellik (University of Michigan, Ann Arbor, MI, USA). HOXA9, HOXB9 and HOXD9 were entered in the Gateway® system (Life Technologies) to generate N-terminally Flag-tagged proteins. The TRAF2 dominant negative (TRAF2-DN) construct was obtained by removing the 87 N-terminal amino acids from the human TRAF2 cDNA. The remaining TRAF2 coding sequence (amino acid residues 88–501) was amplified from the pDEST-GST(Nter)-TRAF2 expression plasmid (22) and inserted into the pDON-233 vector using the Gateway® BP recombination reaction (attB1F primer: GGGGAC AACTTTGTACAAAAAAGTTGGC; attB2R primer: GGGGACAACTTTGTACAAGAAAGTTGGGTA). By Gateway® LR recombination cloning, TRAF2-DN was then transferred into the pDEST-Flag(Nter) destination plasmid resulting in an expression plasmid encoding TRAF2-DN protein tagged with an N-terminal Flag-tag. Pre-tested shRNA constructs from the MISSION® TRC2.0 shRNA library (Sigma-Aldrich) were used in knockdown experiments. The constructs have unique, non-overlapping homology with all target gene transcripts described in http://www.ncbi.nlm.nih.gov/gene. The results shown were obtained with constructs (TRCN0000)234978-82 for HOXA1 (sh-#1-5, respectively), and (TRCN0000) 373433/373443 for TRAF2 (sh-#7/8). TRAF2 shRNA constructs (46) were a kind gift from Dr Tse-Hua Tan (National Health Research Institute, Zhunan, Taiwan). The non-targeting hairpin control SHC002 (Sigma-Aldrich) was used as a negative control. IκB super repressor (IκB-SR) expression plasmid (47) was a kind gift from Dr John Ashton (University of Rochester, New York, USA).

Luciferase assays

MCF10A cells seeded in 24-well plates (2.5×10^5 cells per well) were transfected with 250 ng of luciferase reporter plasmid, 250 ng of the expression plasmids and 50 ng of constitutive reporter plasmid pCMV-LacZ for luciferase ac-

tivity normalization. Empty vector was added when needed so that all transfection reactions contained a total amount of 1 μg of DNA. Twenty-four hours after transfection, cell lysis and enzymatic activity analysis were performed with the β-gal Reporter Gene Assay chemiluminescent (Roche #11758241001) and the Luciferase Reporter Gene Assay high-sensitivity (Roche #11669893001) kits following manufacturer's instructions. For each transfection, the constitutively active pCMV-LacZ reporter was used as an internal standard reporter to avoid experimental variations due to transfection efficiency. The relative luciferase activity was calculated as a luciferase/β-galactosidase ratio. Results are presented as means of three biologically independent duplicates.

ELISA

MCF10A and MCF7 cells seeded in 6-well plates (6.0×10^5 and 4.0×10^4 cells per well respectively) were transfected with 500 ng expression plasmid and 2 μg total DNA. Medium supernatant was collected 48 h post-transfection. Cells were rinsed with phosphate buffered saline (PBS) and lysed in IPLS lysis buffer including Tris–HCl pH 7.5 20 mM, 120 mM NaCl, 0.5 mM ethylenediaminetetraacetic acid, 0.5% NP40, 10% glycerol and protease inhibitor (#11873580001, Roche). IL-8 levels were quantified using the BD OptEIA Human IL-8 ELISA Set (BD Bioscience, East Rutherford, New Jersey, USA) following manufacturer's instructions. Total protein levels were quantified with a Bicinchoninic Acid Assay (BCA) kit (Pierce). Results are presented as means of three biologically independent duplicates. In each experiment, the IL-8 level/protein ratio is calculated as a percentage of the control.

Western blotting

MCF10A and MCF7 cells seeded in 6-well plates (6.0×10^5 and 4.0×10^4 cells per well respectively) were transfected as described above. Twenty-four hours after transfection, or after TNFα addition where stated, cells were washed with PBS and lysed with IPLS lysis buffer. Cell lysates were cleared by centrifugation for 5 min at 500 g and the supernatant was collected. Proteins were boiled in the presence of loading buffer, again centrifuged as above, loaded on SDS-PAGE, transferred on nitrocellulose membrane and processed for detection of specific proteins using antibodies against TAB2 (Cell Signaling #3745), TAB3 (Cell Signaling #14241), p-TAB2 (Ser372) (Cell Signaling #8155), IKKα (Cell Signaling #2682), IKKβ (Cell Signaling #2370), p-IKKα/β (Ser176/180) (Cell Signaling #2697), IκBα (Cell Signaling #4814), p-IκBα (Cell Signaling #2859), p65 (Cell Signaling #8242), p-p65 (Ser536) (Cell Signaling #3033), FLAG (Sigma-Aldrich #F1804), GST (Sigma-Aldrich #G7781), β-actin (anti-β-actin-HRP, Sigma-Aldrich #A3854). The secondary antibodies used were goat anti-mouse IgG-HRP (Cell Signaling #7076) and goat anti-rabbit IgG-HRP (Cell Signaling #7074). Results are presented as a representative example of three biologically independent repetitions of the experiment.

Immunofluorescence

MCF10A cells seeded on glass coverslips in 24-well plates (5.0×10^4 cells per well) were transfected as described above. Twenty-four hours after transfection, or after TNFα addition when stated, cells were fixed for 10 min in 4% paraformaldehyde (PFA). Coverslips were then sequentially incubated with PBS-Triton X-100 for 5 min, and with antibodies against p65 (SantaCruz Biotechnology #sc-372), FLAG (Sigma-Aldrich #F1804) or GST (Sigma-Aldrich #G7781) diluted in PBS–BSA 3% for 1 h. Secondary antibodies anti-rabbit-AlexaFluor-555 (Cell Signaling #4413) and anti-mouse-AlexaFluor-488 (Cell Signaling #4408) were next incubated in PBS–BSA 3% for 1 h. Nuclei were stained with DAPI and coverslips were mounted with Vectashield medium (Vector Laboratories, Cambridgeshire, UK). Results are presented as a representative example of three biologically independent repetitions of the experiment.

Bimolecular fluorescence complementation

COS7 cells seeded on glass coverslips in 24-well plates (1×10^5 cells per well) were transfected with 100 ng of pDEST-VC155(Nter)-HOXA1 (WT or mutant) and 100 ng of pDEST-VN173(Nter)-interactor (RBCK1 or TRAF2). Twenty-four hours after transfection, cells were fixed with 4% paraformaldehyde for 30 min, rinsed three times with PBS and once in TBS containing 0.1% Triton X-100. Glass coverslips were mounted in Vectashield®-DAPI medium. Results are presented as a representative example of three biologically independent repetitions of the experiment. Quantification was performed using the ImageJ software.

Focus formation assay

MCF7 cells seeded in 6-well plates (2×10^5 cells per well) were transfected as described above. Medium was changed every 3 days. After 2 weeks, cultures were washed with PBS and foci were counted under a binocular. Results are presented as three biologically independent repetitions of the experiment.

MTT assay

MCF10A cells seeded in 96-well plates (5×10^3 cells per well) were transfected as described above and medium was changed 24 h after transfection. After 72 h of culture, cells were incubated for 3 h in culture medium supplemented with 0.5 mg/ml 3-(4,5-dimethylthiazolyl-2)-2,5 diphenyltetrazolium bromide (MTT) (Sigma-Aldrich #M2128). Plates were centrifuged for 15 min at 1000 *g*, supernatant was cleared and 200 μl DMSO (Sigma-Aldrich #D2438) was added to dissolve the formazan precipitate. Global cell growth was assessed by measuring the absorbance at a wavelength of 560 nm with background subtraction at 670 nm. Results are presented as means of three biologically independent repetitions of triplicates.

Affinity co-precipitation

HEK293T cells were seeded in 6-well plates (7×10^5 cells per well) and were transfected with 500 ng of pDEST-

Flag(Nter)-HOXA1 (wild-type or mutant) and 500 ng of pDEST-GST(Nter)-interactor (RBCK1 or TRAF2). Fourty-eight hours post-transfection, cells were rinsed with PBS and lysed in lysis buffer. Cell lysates were cleared by centrifugation for 5 min at 500 g and the cleared lysates were incubated over-night on glutathione-agarose beads (Sigma-Aldrich #G4510). The expression of Flag-tagged, GST-tagged proteins and β-actin was verified by western blot before starting the co-precipitation experiments. After overnight incubation of the proteins on glutathione beads, proteins attached to the beads were dissociated from the beads and loaded on SDS-PAGE, transferred on nitrocellulose membrane and processed for detection of Flag-tagged proteins. The intensity of the bands was quantified using ImageJ software (http://imagej.nih.gov) and the signal obtained for each Flag-HOXA1 fusion co-expressed with native GST was subtracted from the signal obtained with that Flag fusion co-expressed with GST-RBCK1 or GST-TRAF2. Results are a representative example of three biologically independent repetitions of the experiment. Quantification was performed using the ImageJ software.

Imaging

For p65 translocation assays, slides were analyzed by confocal microscopy (LSM 710, Zeiss). Images from BiFC and for the cellular relocalization of HOXA1 in presence of RBCK1, TRAF2 and TNFα were obtained by fluorescence microscopy (Axioskop 2, Zeiss). Foci were observed under a binocular (Leitz) and pictures were taken with a Fujifilm Finepix S1 pro camera.

Statistical analysis

For the bio-informatic analyses in Figure 1 and Table 1, HOXA1 mRNA expression was correlated to mRNA expression of other genes using a 2 log Pearson test. The significance of a correlation is determined by $t = R/\mathrm{sqrt}((1-r\wedge 2)/(n-2))$, where R is the correlation value and n is the number of samples. Distribution measure is approximately as t with n-2 degrees of freedom (see http://vassarstats.net/rsig.html for details). Pathway enrichment analysis on HOXA1-correlating genes was performed using the R2 KEGG Pathway Finder and standard settings, the NF-κB signaling pathway (ko04064) is as defined by KEGG (http://www.genome.jp/kegg/). KEGG pathway enrichment was calculated using a 2×2 contingency table analysis, or chi-square test with continuity correction. The P-value represents the significance of over-representation of the pathway in the dataset. $P < 0.05$ was considered statistically significant, unless otherwise stated.

All statistical analyses for lab experiments were performed using the JMP11 software. Data from Luciferase and ELISA assays were transformed as log(10) values prior to the analysis. Results from Luciferase Assays were analyzed with a Tukey HSD test to compare grouped conditions whereas a Dunnett test was performed to compare individual conditions. ELISA results were analyzed with a bilateral one sample test for the mean. Results from MTT, quantification of BiFC and quantification of Affinity co-precipitation were analyzed with a unilateral one sample test for the mean.

RESULTS

HOXA1 expression profiling analysis of public breast cancer datasets

While characterizing the HOXA1 interactome, a set of interactors corresponding to TNF-associated proteins was identified and validated by additional protein–protein interaction assays (22). The validation of the direct interaction between HOXA1 and RBCK1 and TRAF2 led us to hypothesize that HOXA1 might by functionally linked to the TNF/NF-κB-elicited signaling.

HOXA1 and NF-κB have both been associated to breast cancer development. To determine to what extent HOXA1 expression could be correlated *in vivo* to genes involved in the NF-κB functional network, we analyzed breast cancer datasets corresponding to genome-wide expression profiles. To this end, we downloaded and selected mRNA expression data of breast cancer patient cohorts in the public domain from the NCBI GEO depository using the R2 genomics analysis and visualization platform as described in 'Materials and Methods' section. We examined 15 breast cancer datasets in detail. We first collected all genes whose mRNA expression was significantly correlated to that of HOXA1. To obtain insight into signal transduction pathways within this collection, we subjected these genes to a KEGG pathway search. Table 1 shows that the NF-κB pathway was significantly over-represented within the HOXA1-correlating genes in 12 of 15 datasets analyzed, more often than any other signaling pathway. For the largest dataset, Bertucci-266, 67 of the 87 NF-κB pathway genes expressed in tumor samples from this cohort were significantly associated with HOXA1 expression (Figure 1). This suggests an association with HOXA1 of almost the whole NF-κB signal transduction network. The pattern from Bertucci-266 was repeated in the other datasets: of 87 NF-κB pathway genes with significant negative or positive correlation to HOXA1 expression, 54 were consistently positively ($n = 50$) or negatively ($n = 4$) associated with high HOXA1 mRNA expression in 6 or more of the 12 datasets (Supplementary Table S1 and Supplementary Figure S1). Notably, NF-κB-activating ligands and cell surface receptors of all the different NF-κB upstream signaling routes are represented within these 50 positively correlated genes. As are the transcriptional target genes from all different NF-κB downstream effector pathways.

The 12 breast cancer datasets we analyzed are representative of the various breast cancer studies in the public domain. They have very different compositions with regard to clinical grade, (molecular) subtype, tissue site, patient age, etc. In addition, they were performed on three different array platforms. We therefore propose that the results observed are very robust.

We are aware that the NF-κB pathway contains signaling nodes that depend on protein modification or translocation, especially in the intermediate signaling routes, that cannot be detected using mRNA expression profiling. However, we observe a universal positive correlation with the NF-κB extracellular ligands and receptors, and a predominantly positive correlation with the NF-κB transcriptional target genes, that is consistent in the majority of the 12 ex-

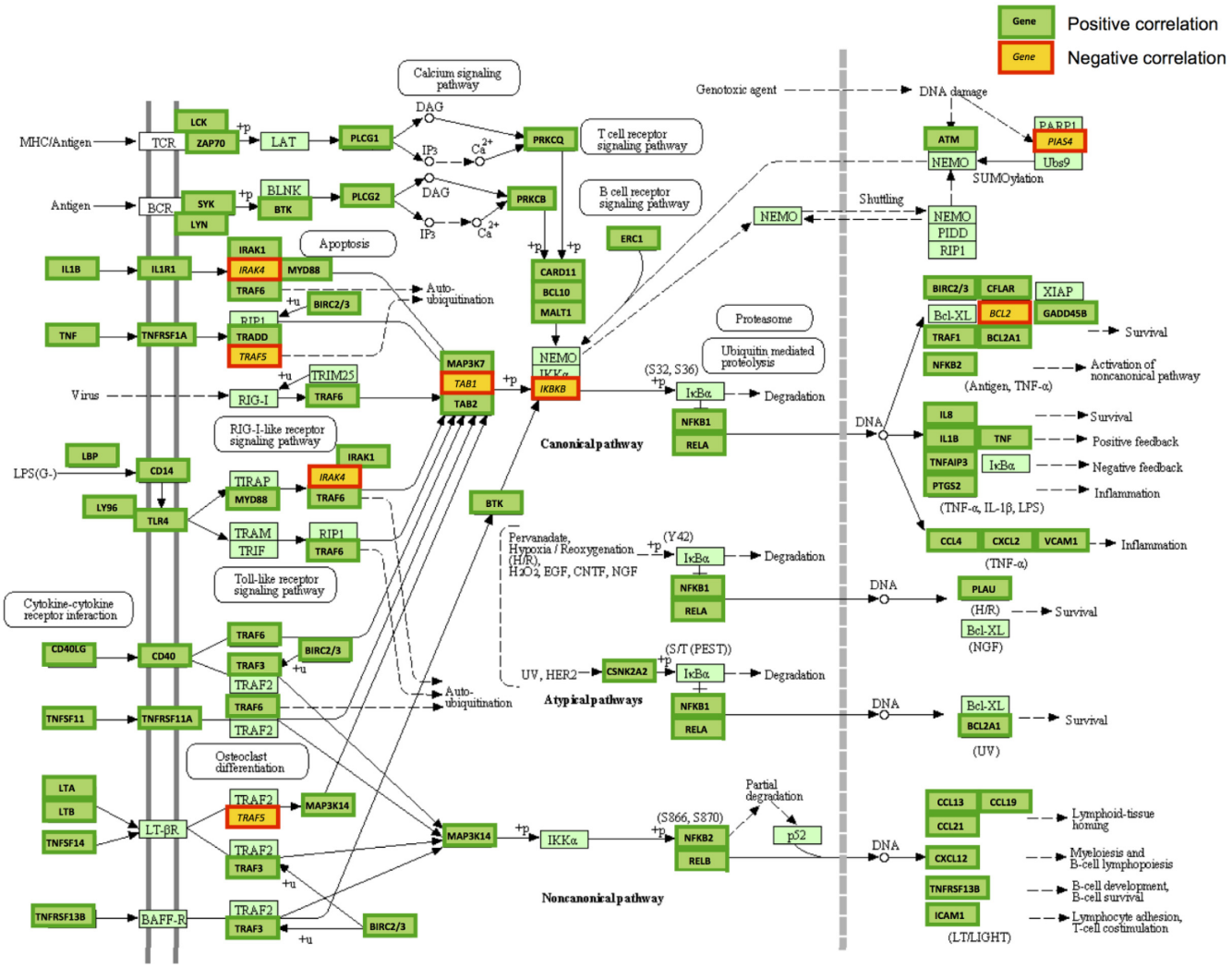

Figure 1. NF-κB pathway genes with correlation to HOXA1 expression in breast cancer. Graphical overview of the NF-κB pathway showing pathway genes with a significant correlation to HOXA1 expression in the Bertucci-266 dataset. The KEGG NF-κB pathway graph with constituent genes (in pale green boxes with narrow border) is overlaid with boxes representing positively or negatively correlating genes (gene name on a green background with thick green border, or on a yellow background with thick red border, respectively). More details on correlations are in Table 1. The overview shows an almost comprehensive positive correlation with HOXA1 mRNA expression, strongly suggesting that the NF-κB pathway is activated by HOXA1 in breast cancer cells.

pression datasets we analyzed. Together, this strongly suggests that the NF-κB pathway is activated in the presence of high HOXA1 expression in breast cancer cells.

HOXA1 triggers the activation of NF-κB in a specific and transcription-independent manner

To first address the ability of HOXA1 to stimulate the NF-κB pathway, we co-transfected human mammary epithelial cells MCF10A with a NF-κB reporter construct containing five copies of a NF-κB responsive element (PGL4.32[luc2P/NF-κB-RE/Hygro], hereafter referred to as 'NF-κB reporter' (39) (Figure 2A) and a HOXA1 expression plasmid. This reporter assay revealed that HOXA1 expression triggered a 4-fold increased activity of the NF-κB reporter. This HOXA1-mediated activation of the NF-κB reporter appeared to be specific since other HOX proteins like HOXA2, HOXA9, HOXB9 and HOXD9 were also tested and could not significantly stimulate the reporter (Figure 2B). The specific effect exerted by HOXA1 on the NF-κB reporter was further confirmed in a loss-of-function model by transfecting MCF7 cells with different shRNAs directed against HOXA1 (sh-HOXA1 #1 to #5). sh-HOXA1 #2 and #3 significantly diminished both the level of the HOXA1 protein and the activity of the NF-κB reporter, demonstrating that the activity of NF-κB reporter is enhanced by HOXA1. sh-HOXA1 #4 and #5 also provoked a slight decrease in HOXA1 abundance and NF-κB reporter activity, although this did not reach statistical significance (Figure 2C).

To determine whether the positive effect exerted by HOXA1 was dependent on the transcriptional activity of the protein, both wild-type and mutant proteins were used on a HOXA1 target reporter derived from the *EPHA2* gene, pML-EPHA2-r4-luc (hereafter referred to as 'HOXA1 re-

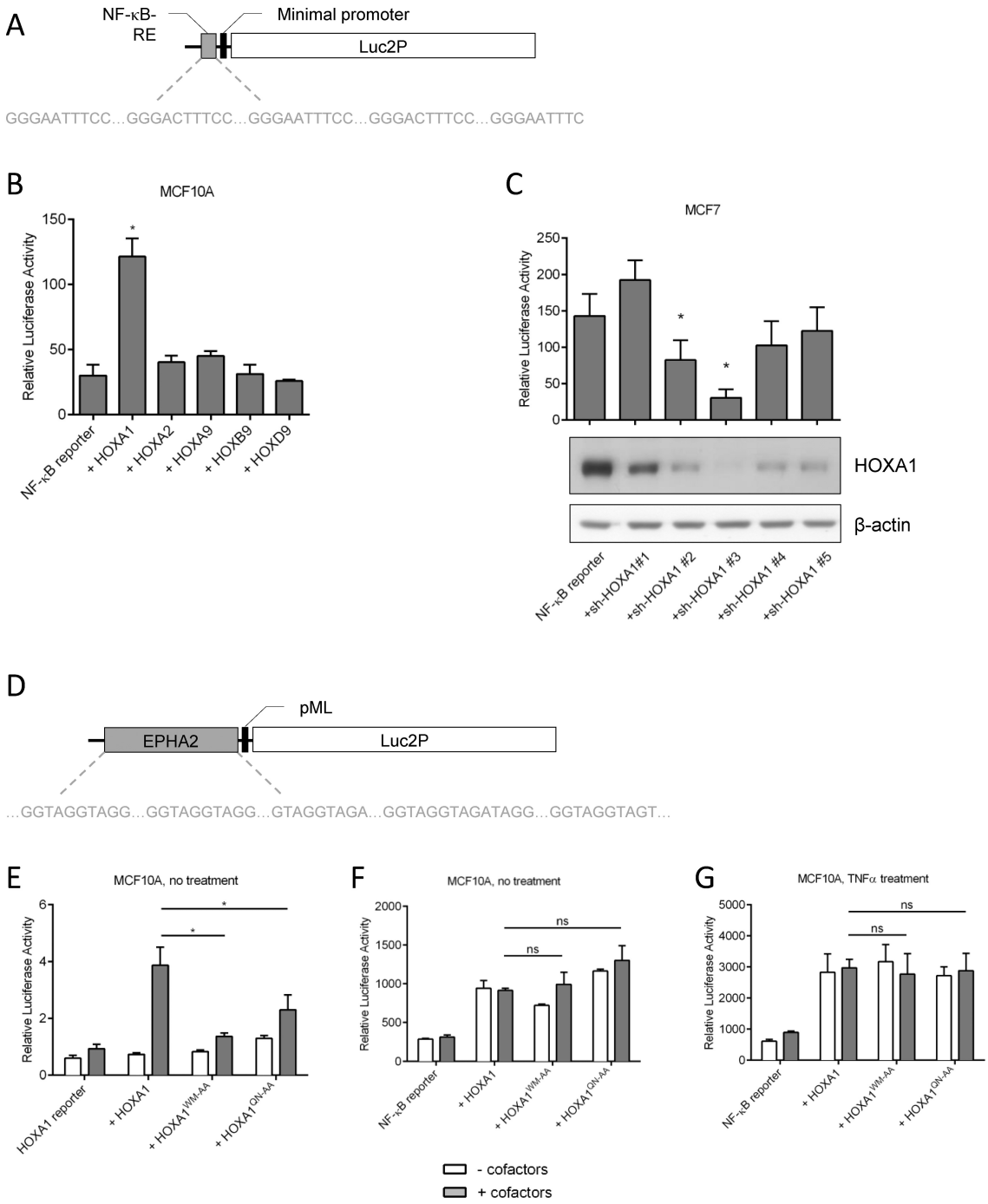

Figure 2. Transactivation assays on both NF-κB- and HOXA1-responsive reporters. (**A**) The NF-κB reporter (PGL4.32[luc2P/NF-κB-RE/Hygro]) consists in a luciferase reporter gene *Luc2P* controlled by five copies of a 10-nt NF-κB responsive element corresponding to p65 binding sites (GGGAATTTCC or GGGACTTTCC). (**B**) The specificity of HOXA1 in activating the TNF/NF-κB pathway was assessed using the NF-κB reporter and HOXA1, HOXA2, HOXA9, HOXB9 and HOXD9 expression plasmids in the human mammary epithelial cell line MCF10A. (**C**) The involvement of HOXA1 in NF-κB activation was assessed in a loss-of-function model by using sh-RNAs directed against HOXA1 in human breast cancer MCF7 cells. The HOXA1 protein level was analyzed by western blot, and the NF-κB activity was quantified by reporter Luciferase assay. (**D**) The HOXA1 reporter (pML-EPHA2-r4-luc) consists in a luciferase reporter gene *Luc2P* controlled by 5 HOX-PBX binding sites defining the *EPHA2* gene r4 enhancer (40). (**E**) The ability of HOXA1 to activate the HOXA1 reporter was assessed in MCF10A cells. As controls, transcriptionally inactive HOXA1$^{WM\text{-}AA}$ and HOXA1$^{QN\text{-}AA}$ mutant proteins were tested. Expression plasmids encoding HOXA1 (wild-type, HOXA1$^{WM\text{-}AA}$ or HOXA1$^{QN\text{-}AA}$) were transfected with or without expression plasmids for the TALE cofactors PREP1 and PBX1. (**F**) Reporter assays performed in MCF10A cells using the NF-κB reporter reveal that transcriptionally inactive HOXA1 variants (HOXA1$^{WM\text{-}AA}$, HOXA1$^{QN\text{-}AA}$) are able to stimulate NF-κB activity. (**G**) Similar experiments as in (**F**) were performed in MCF10A cells with TNFα addition (25 ng/ml for 24 h). Results are presented as a luciferase/β-galactosidase ratio (relative luciferase activity) and correspond to the means of three biologically independent duplicates ± SEM. Statistical analysis was performed (B and C) with reference to the condition involving the NF-κB reporter alone (NF-κB reporter) as control or (E-G) with comparisons between groups (*$P < 0.0001$; ns = not significant).

Table 1. Significant enrichment of the NF-κB pathway among HOXA1-correlating genes in breast cancer datasets

Dataset		KEGG NFkB Pathway				Dataset		
Name	Size	Representation	Genes correlating	Genes total	*P* value	Platform	Depository	PMID
Black	107	Over	28	85	$2.6 \cdot 10^{-4}$	Affymetrix U133P2	GSE36771	**
Bertucci	266	Over	67	87	$1.5 \cdot 10^{-9}$	Affymetrix U133P2	GSE21653	20490655
Booser	508	Over	62	81	0.08	Affymetrix U133A	GSE25066	21558518
Bos	204	Over	52	86	$2.7 \cdot 10^{-5}$	Affymetrix U133P2	GSE12276	19421193
Chin	124	Over	34	81	$4.9 \cdot 10^{-5}$	Affymetrix U133A	*	17157792
Clynes	121	Over	37	87	$1.1 \cdot 10^{-8}$	Affymetrix U133P2	GSE42568	23740839
EXPO	351	Over	40	85	$2.5 \cdot 10^{-3}$	Affymetrix U133P2	GSE2109	**
Iglehart	123	Over	26	85	$2.6 \cdot 10^{-3}$	Affymetrix U133P2	GSE5460	18297396
Jonsdottir	94	Over	37	83	$7.5 \cdot 10^{-7}$	Illumina HWG6V3	GSE46563	24599057
Minn	96	Over	33	78	$6.2 \cdot 10^{-4}$	Affymetrix U133A	GSE2603	16049480
Servant	343	Over	15	84	0.38	Illumina HWG6V3	GSE30682	22271875
Smid	210	Over	52	86	$3.8 \cdot 10^{-6}$	Affymetrix U133P2	GSE29271	**
Sotiriou-1	120	Over	25	85	$6.0 \cdot 10^{-3}$	Affymetrix U133P2	GSE16446	21422418
Sotiriou-2	198	Under	19	80	0.92	Affymetrix U133A	GSE7390	17545524
Wang	286	Over	48	81	$3.4 \cdot 10^{-3}$	Affymetrix U133A	GSE2034	15721472

HOXA1 mRNA expression was correlated to all KEGG NF-κB pathway genes in 15 public breast cancer datasets. Genome-wide expression profiling datasets of breast cancer patients available in the public domain were downloaded, selected and analyzed in R2 as described in the 'Materials and Methods' section. The first two columns represent dataset name and sample size. Columns 3–6 represent the KEGG NF-κB pathway: over- or under-representation, amount of genes correlating, amount of genes in the pathway expressed in the dataset and a *P*-value, respectively. The *P*-value represents the significance of over-representation of the pathway in the dataset (results from a 2 × 2 contingency table analysis, or chi-square test with continuity correction, significance cut-off $P < 0.05$). With a $P < 0.01$ cut-off, the same 12 sets showed NF-κB pathway enrichment, but with ∼20% fewer correlating genes. Columns 7–9 represent dataset platform, NCBI GEO GSE number and PubMed identifier, respectively. *ArrayExpress E-TABM-158. **Studies not yet published. The KEGG NF-κB pathway is significantly over-represented within HOXA1-correlating genes in 12 of 15 breast cancer datasets. For 7 of these 12, the NF-κB pathways was among the top 10 over-represented KEGG pathways. Only the Sotiriou-198 dataset shows an under-representation of NF-κB pathway genes.

porter') (40) (Figure 2D). The HOXA1$^{WM\text{-}AA}$ variant has a substitution in the hexapeptide which makes the protein unable to interact with cofactors like PBX1 (15). As already mentioned, PBX1 has appeared to be a crucial cofactor for the transcriptional activity of HOXA1 on well-characterized target enhancers. The integrity of the HOXA1 hexapeptide has also been shown necessary to the developmental and oncogenic HOXA1 functions (43). HOXA1$^{QN\text{-}AA}$ harbors a substitution in the homeodomain which impairs DNA binding (43). In MCF10A cells, both the HOXA1$^{WM\text{-}AA}$ and HOXA1$^{QN\text{-}AA}$ mutant proteins, failed to activate the HOXA1 reporter as previously described (40). This therefore confirms these mutants as transcriptionally inactive (Figure 2E). Surprisingly, all HOXA1 versions enhanced the activity of the NF-κB driven reporter, supporting that HOXA1 could act on the pathway in a transcription-independent manner. Moreover, addition of PBX1 or the alternative TALE HOXA1 cofactor PREP1, which normally allow HOXA1 to fully activate the HOXA1 reporter (43) had no effect on the activation of the NF-κB reporter by HOXA1 (Figure 2F).

Similar results were observed upon stimulation of the pathway by TNFα addition (Figure 2G). The TNFα-mediated activation of the NF-κB reporter was about six times higher in combination with HOXA1 than without HOXA1. Since NF-κB can also be activated upon stimulation by other cytokines, the same experiment was performed by treating the cells with IL-1β, leading to similar results as with TNFα addition (data not shown). This together supports that HOXA1 activity synergized with cytokine-mediated activation of NF-κB.

To better understand at which level HOXA1 exerts its influence in the TNF/NF-κB signaling cascade, MCF10A cells were co-transfected with expression plasmids for HOXA1 and a non-degradable variant of IκBα (IκBα S32/36A, hereafter called 'IκB-SR') which acts as a repressor of the pathway by preventing NF-κB nuclear translocation (47,48). The HOXA1-mediated activation of the NF-κB reporter was fully suppressed by IκB-SR (Figure 3A), as was also the TNFα-triggered activation of the reporter (data not shown). This therefore demonstrates that HOXA1 acts upstream of IκBα in the signaling cascade.

The ability of HOXA1 to enhance TNFα-mediated NF-κB activation was further evaluated by investigating the phosphorylation status of NF-κB signaling proteins upon TNFα stimulation in the presence or in the absence of HOXA1. MCF10A cells were transfected with a vector coding for HOXA1 or an empty vector as negative control, and were treated with TNFα 24 h later. The cells were harvested at different time-points to evaluate the levels of both total and phosphorylated TAB2 (Ser372), IKKα/β (Ser176/180), IκBα (Ser32) and p65 (Ser536) using western blot analysis. Whereas whole protein levels of TAB2, TAB3, IKKα/β, IκBα and of p65 were similar between cells transfected for HOXA1 or with the negative control, expression of HOXA1 led to increased levels of phosphorylated TAB2 (Ser372), phosphorylated IKKα/β (Ser176/180), phosphorylated IκBα (Ser32) and phosphorylated p65 (Ser536)

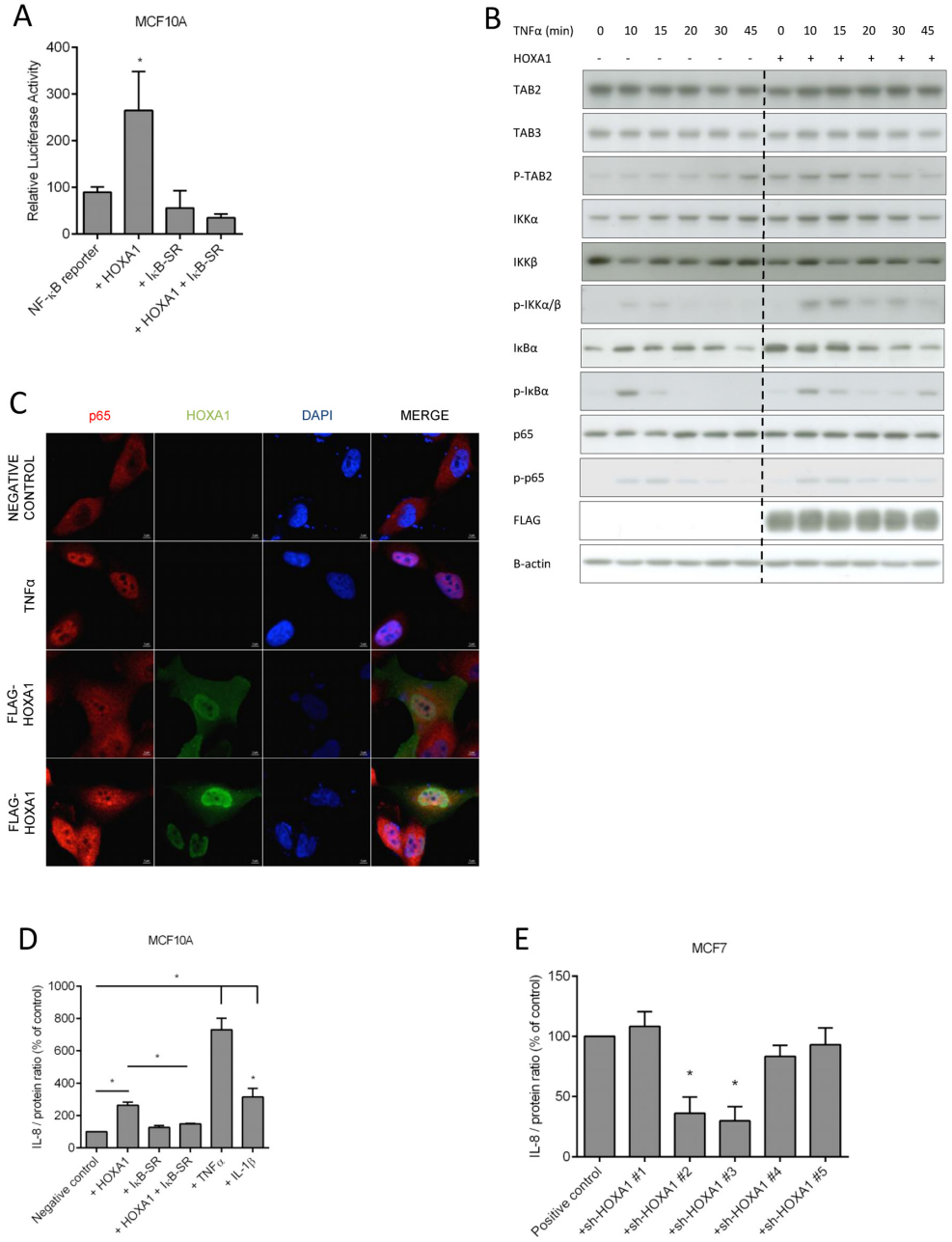

Figure 3. Effect of HOXA1 on the NF-κB pathway. (**A**) The effect of a super repressor version of IκB (IκB-SR) on the HOXA1-mediated activation of the NF-κB reporter was assayed in MCF10A cells. Results are presented as a luciferase/β-galactosidase ratio (relative luciferase activity) and correspond to the means of three biologically independent duplicates ± SEM. Statistical analysis was performed with reference to the condition involving the NF-κB reporter alone (NF-κB reporter). (**B**) Western blot showing TAB2, TAB3, p-TAB2 (Ser372), IKKα, IKKβ, p-IKKα/β (Ser176/180), IκBα, p-IκBα (Ser32), p65 and p-p65 (Ser536) proteins from MCF10A cells transfected with a FLAG-HOXA1 expression plasmid or with a negative control, and treated with TNFα (25 ng/ml) for 0, 10, 15, 20, 30 or 45 min. A total of 25 ng/ml was chosen from a range of 0, 6.25, 12.5, 25, 50, 75 or 100 ng/ml as the lowest TNFα concentration to give full reporter activation. At this TNFα concentration, reporter activation is comparable between 30 min and 24 h (not shown). A total of 250 ng HOXA1 plasmid was chosen as the optimal transfection dose from a range of 0, 50, 100, 250, 500 or 750 ng as the lowest HOXA1 dose to give full reporter activation (not shown). Detection of β-actin was used as loading control. Bands corresponding to detected proteins were cropped for the sake of presentation but all samples were processed in parallel, being run together on single protein gels. The provided blots are representative of three biologically independent experiments. (**C**) p65 nuclear translocation was analyzed in MCF10A cells by confocal microscopy. The images represent the cellular localization of endogenous p65 (red channel) and FLAG-HOXA1 (green channel) from representative confocal Z-section at 120 times magnification. Cell nuclei were stained with DAPI (blue channel). (**D**) ELISA quantification of IL-8 secretion upon HOXA1, IκB-SR, and HOXA1 and IκB-SR expression, or after TNFα or IL-1β addition to MCF10A cells. IL-8 secretion was normalized to the protein content of the cell-culture well and data were calculated using the mean absorbance of two wells. The negative control was set to 100% and statistical analysis was carried out using the negative control as control level (*$P < 0.0001$). This is a representative experiment of three biologically independent duplicates ± SEM. (**E**) The involvement of HOXA1 in triggering IL-8 secretion was assayed as in (D) using sh-HOXA1 vectors in MCF7 cells. The positive control was set to 100% and statistical analysis was carried out using the positive control as control level (*$P < 0.0001$). This is a representative experiment of three biologically independent duplicates ± SEM.

compared to the negative control upon TNFα stimulation. The phosphorylated forms of TAB2 and IKKα/β were detected earlier and were more abundant in cells expressing HOXA1 compared to cells transfected with the negative control. The phosphorylated forms of IκBα and p65 were detected for a longer period in cells expressing HOXA1 (Figure 3B and Supplementary Figure S2). These results therefore show that HOXA1 could stimulate TAB2, IKKα/β, IκBα and p65 phosphorylation in combination with TNFα.

As mentioned above, NF-κB activation results in nuclear translocation of NF-κB dimers, the most common being p65/p50 dimers. We therefore investigated by immunofluorescence whether HOXA1 could trigger p65 relocalization to the nucleus in MCF10A cells (Figure 3C). Whereas p65 was located in the cytoplasm in cells transfected with an empty vector (negative control), p65 nuclear translocation was observed in cells treated 15 min with TNFα. Cells expressing HOXA1 displayed both a cytoplasmic and a nuclear p65 localization. This confirms that the HOXA1-dependent NF-κB activation can be associated to p65 nuclear translocation.

Finally, we evaluated the ability of HOXA1 to stimulate IL-8 secretion as a downstream effect of NF-κB target gene activation. Transfection of HOXA1 in MCF10A cells provoked a more than 2-fold increase in IL-8 secretion as detected in the culture medium. Similarly, TNFα and IL-1β addition resulted in a high level of IL-8 secretion. As expected, co-expression of HOXA1 and IκB-SR significantly reduced the positive effect of HOXA1 on IL-8 production (Figure 3D). The specificity of HOXA1 to trigger IL-8 secretion was confirmed in a loss-of-function model by transfecting vector coding for sh-HOXA1 in MCF7 cells. As observed for the Luciferase assays, sh-HOXA1 #2 and #3 decreased the HOXA1-related IL-8 levels compared to the positive control corresponding to non transfected cells showing endogenous HOXA1 expression. Transfection of sh-HOXA1 #1, #4 and #5 led to IL-8 levels similar to the positive control (Figure 3E).

Taken together, these data show that HOXA1 can activate NF-κB in a specific and transcription-independent manner, acting upstream of IκB in the signaling cascade and triggering TAB2, IκBα, IKKα/β and p65 phosphorylation, p65 nuclear translocation and NF-κB target gene activation.

The HOXA1-interactors RBCK1 and TRAF2 are epistatic to HOXA1 in modulating the activation of NF-κB

Since RBCK1 and TRAF2 were identified as direct HOXA1 interactors (22), the ability of those proteins to modulate HOXA1 activity on NF-κB was evaluated in MCF10A cells. Activity tests were performed using an NF-κB reporter, with each interactor alone or in combination with HOXA1. RBCK1 did not activate the NF-κB reporter whereas TRAF2 triggered a high increase of its activity. Surprisingly, RBCK1, that is reported in lots of studies as a subunit of the LUBAC complex that stabilizes the TRADD-dependent complex and enhances formation of the IKK complex (24,25), repressed the stimulatory activity of HOXA1 on the NF-κB reporter. In addition, RBCK1 also inhibited the NF-κB reporter activation mediated by TRAF2. This suggests that RBCK1 exerts an epistatic activity toward both HOXA1 and TRAF2 (Figure 4A). These data therefore support the hypothesis that HOXA1 is implicated in the TNF/NF-κB pathway upstream or at the level of RBCK1. Similar results were obtained upon stimulation of the pathway by TNFα (Figure 4B) or IL-1β (Figure 4C). Also, the results observed were similar whether the wild-type HOXA1 or the $HOXA1^{WM\text{-}AA}$ or $HOXA1^{QN\text{-}AA}$ mutants were expressed (data not shown).

Regarding the functional interaction between HOXA1 and TRAF2, HOXA1 did not further enhance the TRAF2-mediated reporter activation that was already fully activated by TRAF2. To assess whether TRAF2 is epistatic to HOXA1 in NF-κB signaling, we generated a dominant negative construct of TRAF2 (hereafter called 'TRAF2-DN') by removing its N-terminal RING finger domain. This abrogates its NF-κB activation capability (49–51). Interestingly, TRAF2-DN inhibited the stimulatory effect of HOXA1 on the NF-κB reporter, as well as the activation exerted by TRAF2 (Figure 4D). Similarly, co-transfection of HOXA1 with vectors coding for sh-RNAs directed against TRAF2 resulted in a decreased ability for HOXA1 to trigger NF-κB activation. (Figure 4E). Since HOXA1 is unable to activate NF-κB in the presence of TRAF2-DN or sh-TRAF2, this suggests that HOXA1 acts upstream or at the level of TRAF2 in the signaling cascade.

Quantification of IL-8 secretion was then performed to deeper characterize the effect of RBCK1 and TRAF2 on the HOXA1-mediated NF-κB activation. As already observed, HOXA1 expression led to increased IL-8 production. Addition of RBCK1, alone or in combination with HOXA1, led to an IL-8 level that was similar to the negative control. Consistent with our observations with the NF-κB reporter, the IL-8 level was greatly increased by TRAF2, whether HOXA1 was co-expressed or not (Figure 4F).

Finally, the influence of RBCK1 and TRAF2 on HOXA1 cellular localization was evaluated by immunofluorescence. In MCF10A cells transfected with HOXA1 only, the protein was exclusively located in the nucleus. Co-transfection of FLAG-HOXA1 and GST-RBCK1 or GST-TRAF2 resulted in both nuclear and cytoplasmic localization of HOXA1. In TNFα-treated cells, HOXA1 was also located in the nucleus and in the cytoplasm of most cells (Figure 5). These observations strongly suggest that HOXA1 is recruited from the nucleus to the cytoplasmic compartment of the cells by RBCK1 and TRAF2 or upon activation of the pathway by TNFα.

In conclusion, our data demonstrate that RBCK1 and TRAF2 have opposite epistatic effects on the HOXA1 activation of the NF-κB pathway and influence the cellular localization of HOXA1. Furthermore, HOXA1 is inhibited by RBCK1 and acts upstream or at the level of both RBCK1 and TRAF2 in the signaling cascade.

The 11-His repeat and the homeodomain of HOXA1 are essential for NF-κB activation

To identify the structural determinants involved in the HOXA1-mediated activation of NF-κB, we used HOXA1 mutants that were previously generated by random pen-

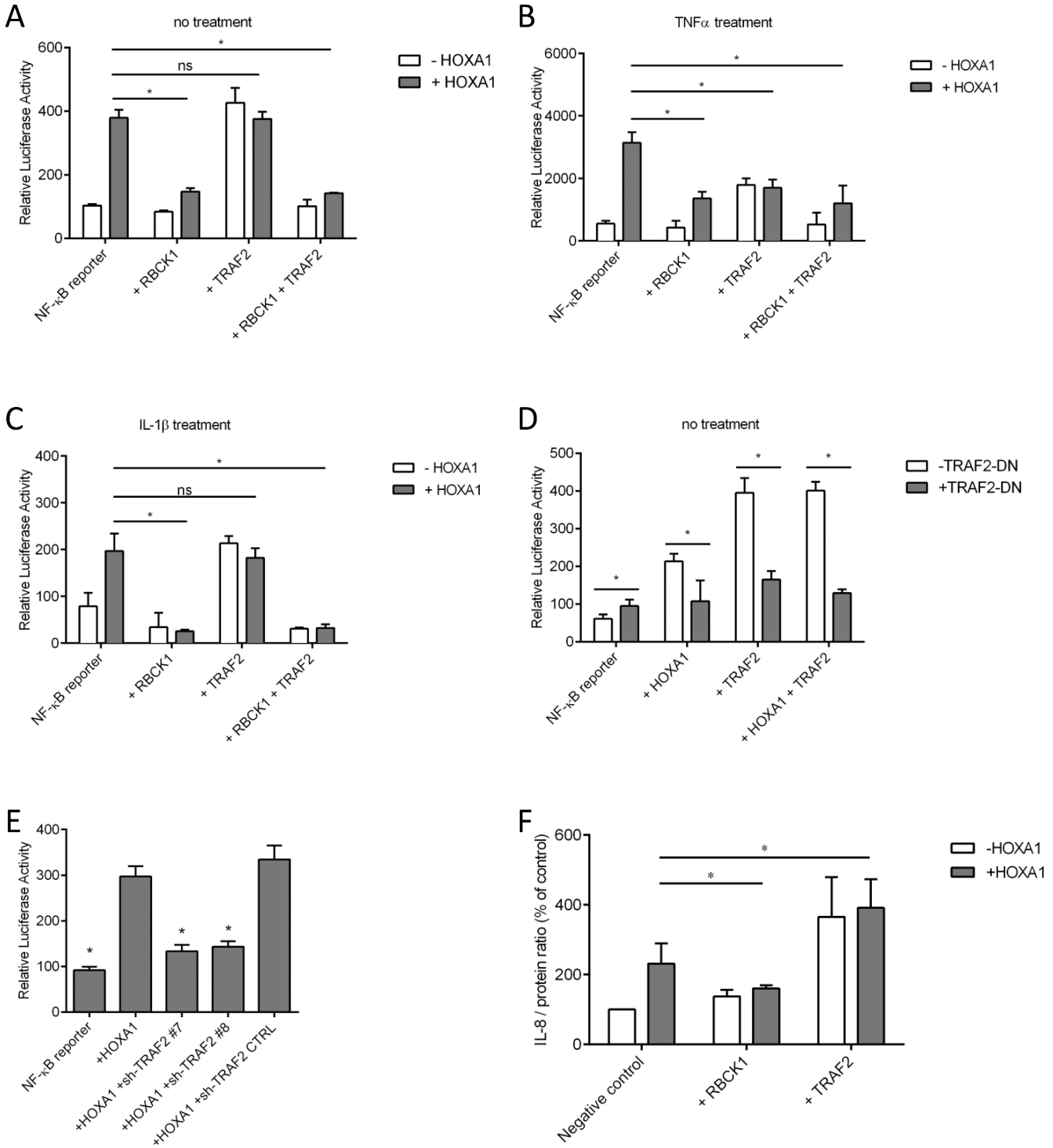

Figure 4. Effect of RBCK1 and TRAF2 on the HOXA1-mediated activation of the NF-κB reporter. (**A**) Activity tests were performed using the NF-κB reporter where each interactor was transfected alone or in combination with HOXA1. Results are presented as a luciferase/β-galactosidase ratio (relative luciferase activity) and correspond to the means of three biologically independent duplicates ± SEM. (**B**) The same experiment was performed after stimulation of the pathway with TNFα. The experiments were performed with 30 min or 24 h TNFα stimulation, with similar results (not shown, see also legend to Figure 3B). (**C**) The same experiment was performed after stimulation of the pathway with IL-1β. (**D**) Effect of a dominant negative version of TRAF2 (TRAF2-DN) on the HOXA1-mediated activation of the NF-κB reporter. (**E**) Activity tests were performed using the NF-κB reporter where HOXA1 was transfected alone or in combination with sh-TRAF2 expression vectors. (**F**) ELISA quantification of IL-8 secretion upon RBCK1, TRAF2 and HOXA1 expression. IL-8 secretion was normalized to the protein content of the cell-culture well and data were calculated using the mean absorbance of two wells. The negative control was set to 100% and statistical analysis was carried out using the negative control as control level (*$P < 0.0001$). This is a representative experiment of three biologically independent duplicates ± SEM. The experiments for (A and D) were not performed at the same time, so variations in cell culture (e.g. passage number, confluence) and/or transfection could be different. All the experiments were performed in MCF10A cells. Data were obtained, processed and represented as in Figure 2. Statistical analysis was carried out (E) with the condition involving the NF-κB reporter alone (NF-κB reporter) as control level, or (A–D; F) using comparisons between groups. (*$P < 0.0001$; ns = not significant).

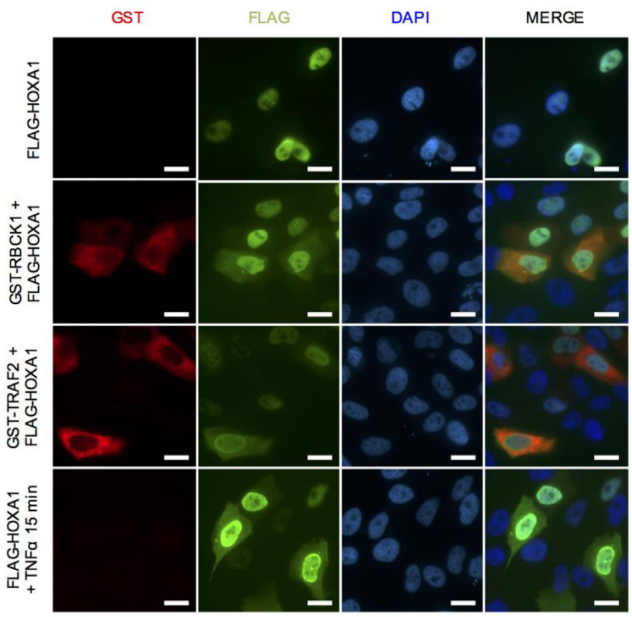

Figure 5. Effect of RBCK1, TRAF2 and TNFα on the HOXA1 intracellular localization. Immunofluorecence was performed after transfection of MCF10A cells with FLAG-HOXA1 alone or in combination with GST-RBCK1 or GST-TRAF2, or upon TNFα treatment (25 ng/ml, 15 min). Scale bars correspond to 0.02 mm.

tapeptide insertion mutagenesis (45). All the insertion mutants activated the NF-κB reporter to similar levels as wild-type HOXA1 (Supplementary Figure S3). Consistent with the results obtained for the transcriptionally inactive HOXA1$^{QN\text{-}AA}$ protein mutated in the homeodomain, HOXA1 insertion mutants P14, P15 and P16, showing a disrupted homeodomain, were not affected in their ability to activate the NF-κB reporter. Interestingly, mutants displaying a loss-of-activity on a HOXA1 reporter (P1, P5, P13, P15, P16, P17) (45) could still activate the NF-κB reporter as efficiently as wild-type HOXA1. This again confirms the transcription-independent activity of HOXA1 in the NF-κB signaling pathway.

We next generated a set of HOXA1 deletion mutants (Figure 6A). Evaluating their expression levels by western blot in the soluble fraction of cell lysates revealed that the HOXA1$^{\Delta Nter}$, HOXA1$^{\Delta 11His}$ and HOXA1$^{\Delta HD}$ proteins were expressed at similar levels as wild-type HOXA1, whereas HOXA1$^{\Delta 77\text{-}205}$ and HOXA1$^{\Delta Cter}$ showed lower expression (Figure 6B).

The HOXA1$^{\Delta Nter}$ and HOXA1$^{\Delta Cter}$ mutants displayed similar activity as the wild-type on the NF-κB reporter (Figure 6C). HOXA1$^{\Delta 77\text{-}205}$ displayed a slightly decreased activity compared to the wild-type which may be caused by it lower expression level. In striking contrast, HOXA1$^{\Delta 11His}$, deleted for the 11-His repeat, and HOXA1$^{\Delta HD}$, devoid of its homeodomain, both lost their ability to activate the NF-κB reporter. However HOXA1$^{\Delta 11His}$ was as active as the wild-type on the HOXA1 reporter (Figure 6D). This therefore demonstrates that HOXA1$^{\Delta 11His}$ has not lost its ability to activate transcription but has lost its capacity to non-transcriptionally modulate the NF-κB pathway. Otherwise, consistent with the known involvement of the homeodomain in DNA binding and activation of transcription, HOXA1$^{\Delta HD}$ could not activate the HOXA1 reporter. The ability of the HOXA1 deletion mutants to activate the NF-κB pathway was again evaluated by testing their capacity to trigger IL-8 secretion. Consistently with their hypoactive effects observed on the NF-κB reporter, HOXA1$^{\Delta 11His}$ and HOXA1$^{\Delta HD}$ caused lower IL-8 secretion levels compared to the wild-type HOXA1 protein (Figure 6E).

Together, these data indicate that both the 11-His repeat and the homeodomain of HOXA1 are important to establish the molecular contacts that initiate the indirect and non-transcriptional HOXA1-mediated NF-κB activation.

HOXA1$^{\Delta 11His}$ and HOXA1$^{\Delta HD}$ show decreased interaction with RBCK1 and TRAF2

We wanted to determine whether a molecular interaction between HOXA1 and RBCK1 or TRAF2 underpins their functional interaction in modulating NF-κB activity, and whether the hypoactive effect of HOXA1$^{\Delta 11His}$ and HOXA1$^{\Delta HD}$ was correlated with a reduced interaction with RBCK1 or TRAF2. This was addressed by affinity co-precipitation assays and Bimolecular Fluorescence Complementation (BiFC).

For the co-precipitation assays, FLAG-tagged wild-type or mutant HOXA1 proteins were co-expressed with GST-tagged RBCK1 or GST-tagged TRAF2 in HEK293T cells. The expression level of FLAG- and GST-tagged proteins was controlled (with β-actin detection as loading control) and the background binding of HOXA1-FLAG or mutant HOXA1-FLAG to the glutathione-agarose beads after co-expression with native GST was low. Although these experiments await further quantification by e.g. titration of input protein, we propose that the HOXA1$^{\Delta 11His}$ and HOXA1$^{\Delta HD}$ mutants appeared to interact less efficiently with both RBCK1 and TRAF2, in comparison to the positive control loaded on the same gel (Figure 7A and B). We realize that our HOXA1 binding experiments are based on HOXA1 over-expression, and would need final confirmation by assays using endogenously expressed HOXA protein. However, the very similar— but opposite effects of endogenous HOXA1 knockdown on NF-κB reporter activity and IL-8 secretion lead us to propose that also endogenous HOXA1 could interact with RBCK1 and TRAF2.

For BiFC, the HOXA1 mutants were fused C-terminally to the C-terminal 155 amino acids of the Venus fluorescent protein (VC155) while TRAF2 and RBCK1 were fused C-terminally to the N-terminal 173 amino acids of the Venus (VN173) as previously described (22). Detection of fluorescence in COS7 cells transfected with the VN173 and VC155 fusion proteins shows that the functional Venus has been reconstituted, indicating that the proteins fused to each Venus moiety interact. As negative controls, we assessed the fluorescence resulting from the expression of unfused Venus moieties in combination with the counterpart fusion proteins. Combining VC155-HOXA1, containing either HOXA1 wild-type or deletion mutants, with unfused VN173 protein led to only low, background fluorescence. Similarly, VN173-RBCK1 and VN173-TRAF2 only provided background fluorescence while co-expressed with un-

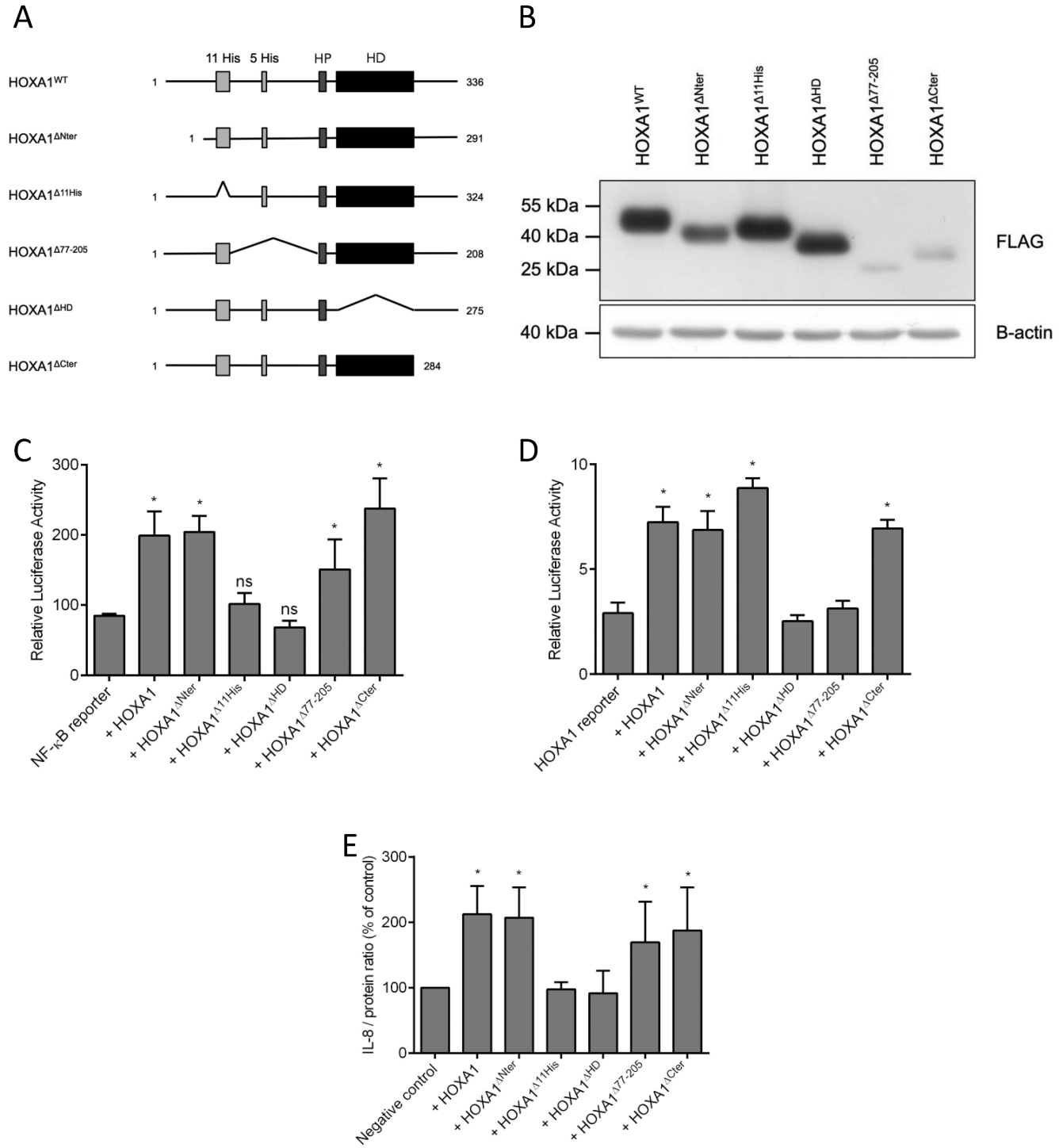

Figure 6. Impact of HOXA1 deletions on NF-κB activation. (**A**) Schematic representation of HOXA1 deletion derivatives. The wild-type (WT) protein contains two functional domains: the homeodomain (HD) and the hexapeptide (HP). It also contains two His rich regions: an 11-Histidine repeat (11-His) at the N-terminal side and a 5-His repeat (5-His) between the 11-His repeat and the hexapeptide. HOXA1$^{\Delta Nter}$ lacks the first 40 amino acids; HOXA1$^{\Delta 11His}$ lacks the complete 11-His repeat; HOXA1$^{\Delta HD}$ lacks the homeodomain; HOXA1$^{\Delta 77\text{-}205}$ lacks the amino acids between the 11-His repeat and the hexapeptide; HOXA1$^{\Delta Cter}$ is devoid of the C-terminal 48 amino acids. (**B**) HOXA1 deletion mutant expression was analyzed by western blot. Samples were centrifuged before use and only the soluble fraction was analyzed on gel. We did not find HOXA1 protein in the insoluble fraction (**C** and **D**) Activity of the HOXA1 deletion mutants on the NF-κB and HOXA1 reporters, respectively. Results are presented as a luciferase/β-galactosidase ratio (relative luciferase activity) and correspond to the means of three biologically independent duplicates ± SEM. (**E**) ELISA quantification of IL-8 secretion upon expression of HOXA1 deletion mutants. Results were obtained as presented in the legend to Figure 3D. All the experiments were performed in MCF10A cells.

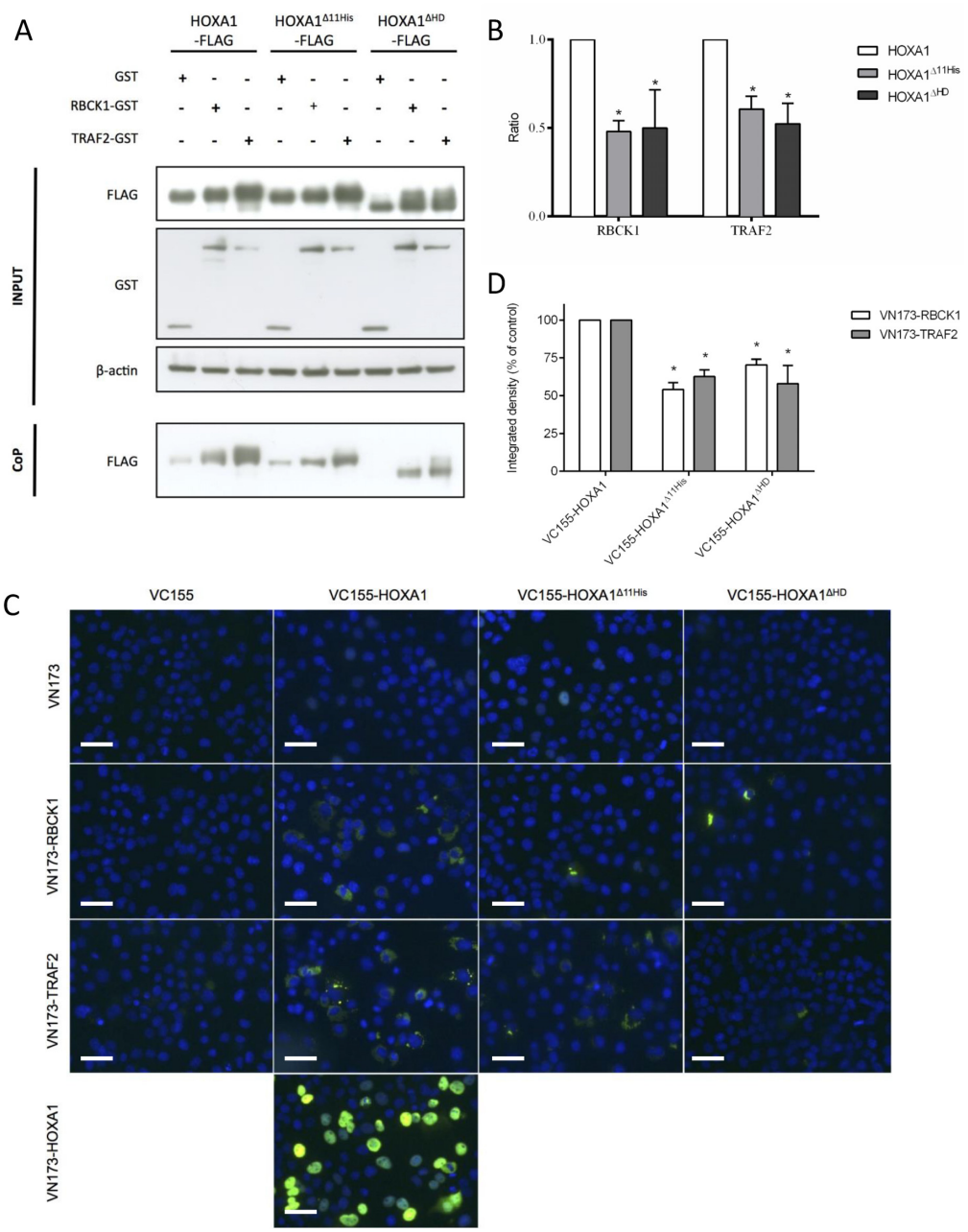

Figure 7. Interaction assays. (**A**) Co-purification of proteins on glutathione-agarose beads. Expression plasmids for FLAG-tagged WT and mutant HOXA1 were co-transfected with GST-tagged RBCK1 and GST-tagged TRAF2 in HEK293T cells. Western blot analysis was used to detect FLAG-tagged HOXA1, RBCK1-GST, TRAF2-GST and β-actin proteins from cell extracts before purification ('Input'). After purification, we retrieved comparable levels of RBCK1-GST and TRAF2-GST from the beads (not shown). Samples were centrifuged before use and only the soluble fraction was analyzed on gel. We did not find HOXA1 protein in the insoluble fraction. Data presented are representative examples; the experiments were performed three times reaching similar results. (**B**) Quantification of the FLAG-tagged Hoxa1 protein bands retrieved from the three co-purification experiments. Results are presented as ratios between the mutant and WT HOXA1 co-precipitation, after subtraction of the signal corresponding to the background co-precipitation obtained with native GST and correspond to means ± SEM ($n = 3$). Values were statistically analyzed using an Unilateral one sample test for the mean (*$P < 0.0001$). (**C**) Bimolecular Fluorescence Complementation assay. COS7 cells were transfected with combinations of expression plasmids for VN173, VC155, VC155-HOXA1, VC155-HOXA1$^{\Delta 11His}$, VC155-HOXA1$^{\Delta HD}$, VN173-RBCK1 or VN173-TRAF2. Upon co-expression of VN173-HOXA1 and VC155-HOXA1, the Venus protein is reconstituted and becomes fluorescent as HOXA1 can dimerize (65). Fluorescence complementation does not occur when unfused VN173 and VC155 are co-expressed. Co-expression of VC155-HOXA1 or VC155-HOXA1 deletion derivatives with unfused VN173 serve as controls for background signal. Co-expression of VC155-HOXA1 or VC155-HOXA1 mutants with VN173-RBCK1 or VN173-TRAF2 reveals that both HOXA1$^{\Delta 11His}$ and HOXA1$^{\Delta HD}$ interact less efficiently with RBCK1 or TRAF2. This is a representative example of three biologically independent experiments. Although the relative expression levels of the three VC155-HOXA1 fusion proteins were not determined in this experiment, we propose that the comparable expression levels of the three native HOXA1 proteins (Figure 6B) suggest that also the VC155-HOXA1 fusions are expressed at similar levels. Scale bars correspond to 0.02 mm. (**D**) BiFC quantification. The integrated density corresponds to the measurement of fluorescence intensity according to the ImageJ software. The integrated density of VC155-HOXA1-VN173-RBCK1 or VC155-HOXA1-VN173-TRAF2 was set to 100% and was used as control level for the statistical analysis (*$P < 0.0001$). Results of three biologically independent repetitions of the experiment were used for quantification.

fused VC155 (Figure 7C). As a positive control, the established HOXA1-HOXA1 interaction assayed with VN173-HOXA1 and VC155-HOXA1 fusions generated a strong signal. Finally, the VC155-HOXA1 deletion mutants co-expressed with VN173-RBCK1 or with VN-173-TRAF2 displayed lower fluorescent signal intensities compared to the wild-type VC155-HOXA1 (Figure 7C) and we quantified this loss of interaction for both deletion derivatives in the BiFC assay (Figure 7D).

Taken together, both interaction assays for HOXA1$^{\Delta 11His}$ and HOXA1$^{\Delta HD}$ indicate that these deletions impaired the capacity of HOXA1 to interact with TRAF2 and RBCK1.

NF-KB activation is crucial for HOXA1 oncogenic activity

As HOXA1 is a human mammary epithelial oncogene, the need for HOXA1 to activate the NF-κB pathway to exert its oncogenic potential was then assessed. Cell-to-cell contacts formed by normal epithelial cells when they reach confluence operate to suppress further cell proliferation. Tumor cells are capable to lose this contact inhibition, giving rise to focus formation (16,52). The ability for endogenous HOXA1 to evade growth suppressors and trigger focus formation was tested by transfecting MCF7 cells with a vector coding for sh-HOXA1. As illustrated in Figure 8A, after two weeks in culture, HOXA1 positive MCF7 cells displayed numerous foci while the downregulation of HOXA1 abrogated focus formation. To next test whether the HOXA1-mediated stimulation of focus formation required the NF-κB pathway, MCF7 cells were transfected with the pathway inhibitor IκB-SR. Most strikingly, MCF7 cells transfected with IκB-SR did not enhance focus formation, just like with the sh-HOXA1 (Figure 8A). This supports that focus formation related to the oncogenic potential of HOXA1 relies on the NF-κB pathway.

It has been previously demonstrated that overexpression of HOXA1 in human mammary epithelial cells leads to an increased proliferation rate (16,53). Its capacity to increase proliferation independently of the NF-κB pathway was then evaluated by transfecting MCF10A cells with a vector coding for HOXA1 alone or in combination with IκB-SR. HOXA1 overexpression led to an increased proliferation rate of the cells, as already demonstrated whereas co-transfection of HOXA1 and IκB-SR did not enhance cell proliferation which was similar to the negative control (Figure 8B). This demonstrates that HOXA1 cannot stimulate the proliferation of human breast cells if the NF-κB pathway is blocked.

In conclusion, activation of the NF-κB pathway is crucial for HOXA1 to mediate oncogenicity.

DISCUSSION

HOX proteins have been extensively studied and by now widespread knowledge exists on their sequence and structure, as well as on their target genes. In contrast, the large range of proteins that HOX transcription factors can be expected to interact with remain scarcely identified. We therefore performed an interactome screen with HOXA1 and significantly ended up with several interactors that are involved in the TNF/NF-κB pathway. In this study, we first demonstrated a highly significant positive correlation between expression of *HOXA1* and of members of the TNF/NF-κB signaling pathway in breast tumor public datasets, including extracellular ligands, receptors, signal transducers and adaptor molecules from different converging signaling routes leading to NF-κB activation. Also the NF-κB transcription factor family members and some of their transcriptional target genes were found in this analysis. In addition to the *HOXA1* and TNF/NF-κB correlation in breast tumor datasets, we demonstrated in cell models, (i) that *HOXA1* can activate NF-κB both independently and in synergy with TNFα stimulation, (ii) that HOXA1 activates NF-κB in a specific and non-transcriptional fashion, (iii) that HOXA1 operates upstream of the NF-κB inhibitor IκB, by triggering TAB2 (Ser372), IKKα/β (Ser176/180), IκBα (Ser32) and p65 (Ser536) phosphorylation and p65 nuclear translocation, (iv) that RBCK1 and TRAF2 influences on the NF-κB response are epistatic to HOXA1 and finally (v) that the 11-His repeat and the homeodomain of HOXA1 are important for the functional interaction between HOXA1 and NF-κB activation as well as for the molecular interaction between HOXA1 and RBCK1 and TRAF2. Finally, we also showed that the HOXA1-mediated cell-proliferation and loss of contact inhibition are abrogated upon NF-κB pathway inhibition. Together our data demonstrate that the HOXA1 transcription factor can fulfill non-transcriptional functions as a stimulator of TNF signaling acting upstream or at the level of both RBCK1 and TRAF2 and leading to NF-κB activation in a context meaningful to breast tumorigenesis.

This study set out using *in silico* data in the public domain. The consistent over-representation of the NF-κB signaling pathway among the signaling routes correlated to HOXA1 expression, and the highly significant positive correlations between most genes in the NF-κB pathway and HOXA1 expression in breast tumor samples suggests a marked implication of HOXA1 in this pathway in the context of breast cancer pathogenesis. HOXA1 has already been associated to breast cancer development in multiple studies. Its forced expression is sufficient to induce the oncogenic transformation of immortalized human mammary epithelial cells to aggressive *in vivo* carcinoma (11,13,53). HOXA1 can also modulate the p44/42 MAP kinase, STAT3 and STAT5B pathways to mediate the oncogenic transformation of human mammary epithelial cells and regulates *Bcl-2*, *hTERT* and *c-Myc*, all genes involved in cancer development (13,53). We previously demonstrated that the overexpression of *HOXA1* in MCF7 human mammary epithelial cancer cells enhanced their proliferation, their anchorage-independent growth and their loss of contact inhibition, which are recognized hallmarks of oncogenesis (16,52,54). The functional connection we highlighted here between HOXA1 and NF-κB is meaningful in the context of breast oncogenesis. Constitutive activation of NF-κB transcription factors p65 and p50 has been widely reported in breast cancers and has been associated with cell survival, proliferation, angiogenesis, metastasis and chemoresistance (55–60). *TRAF2* also has been reported as an oncogene in epithelial cells (37). The existence of cross-talks between NF-κB and other transcription factors and regulatory molecules is also well established for several kinds of

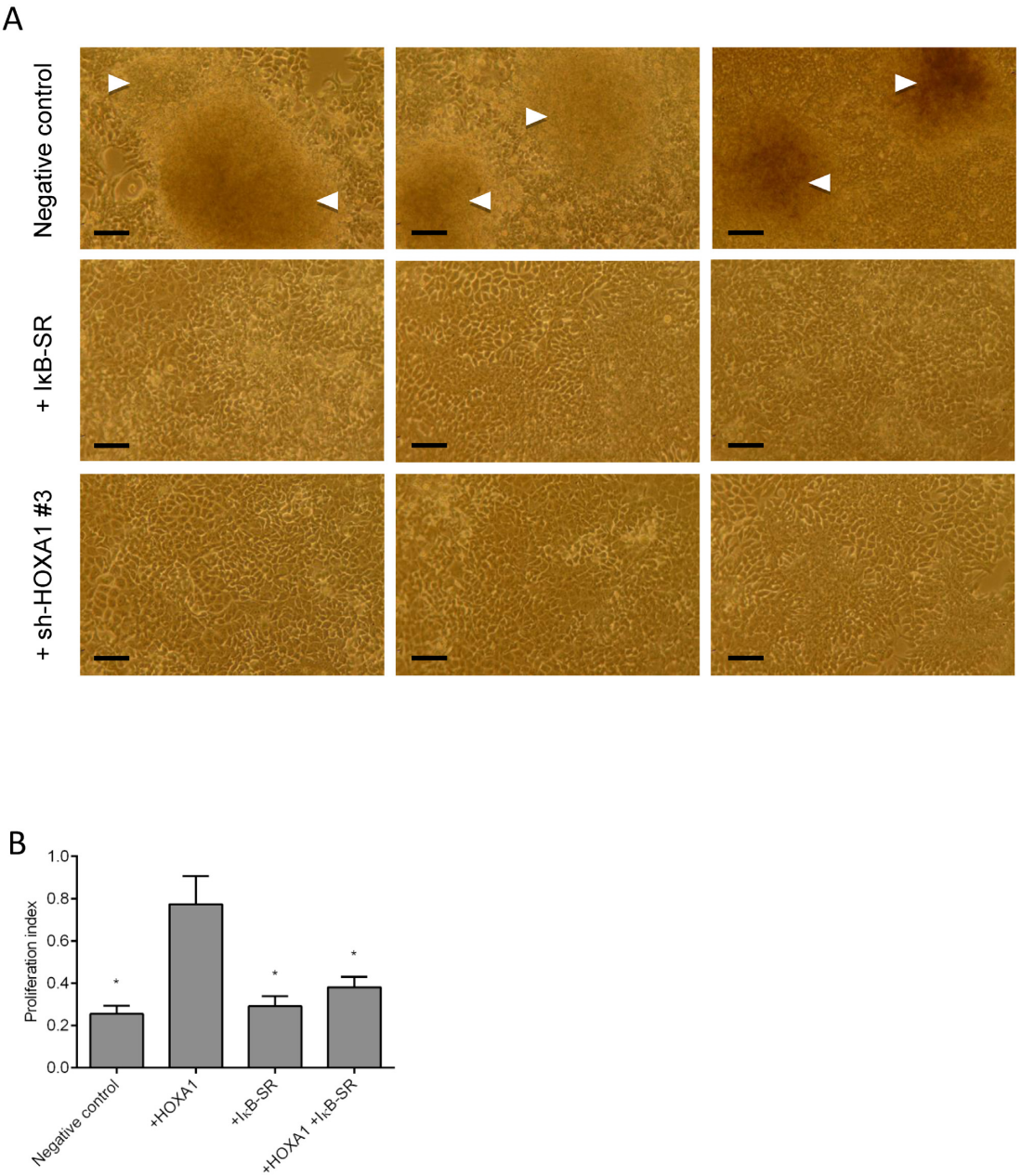

Figure 8. Oncogenicity tests. (**A**) Foci formation assay was performed by transfecting MCF7 cells with empty vector (negative control), IκB-SR or sh-HOXA1 #3. After 2 weeks in culture, foci formation was observed for the negative control (white arrowheads) whereas cells transfected with IκB-SR or sh-HOXA1 did not form foci. Pictures presented were taken from three biologically independent experiments. Scale bar corresponds to 0.02 mm. (**B**) MTT assay was performed by transfection MCF10A cells with HOXA1 alone or in combination with IκB-SR. Global cell growth was determined by MTT assay. Results are presented as a proliferative index obtained by calculating the mean absorbance of each condition and corresponds to the mean of three biologically independent triplicates ± SEM. Statistical analysis was carried out using the 'HOXA1' condition as control level (*$P < 0.0001$).

cancers that display NF-κB activation (61). Therefore, in addition to oncogenic processes and oncogenes which have been shown to be controlled by HOXA1, we suggest here that HOXA1 also activates the NF-κB pathway to promote oncogenesis in mammary epithelial cells.

As mentioned above, RBCK1 (also known as HOIL-1), together with HOIP and SHARPIN, is a part of the LUBAC complex which stabilizes the TRADD-dependent complex and enhances formation of the IKK complex (23–25). While investigating the influence of RBCK1 on the positive effect exerted by HOXA1 on NF-κB, we unexpectedly observed that oppositely to what is generally described in the literature RBCK1 has an inhibitory influence on NF-κB activity which was epistatic to both HOXA1 and TRAF2-mediated stimulation. Using over-expression of HOXA1 or TRAF2, we hereby confirm the ability of the E3 ubiquitin ligase RBCK1 to display the inhibitory effect toward NF-κB which has already been suggested by others (26). In that study, it was demonstrated that RBCK1 physically interacts with TAB2/3 to target them to a proteasome-dependent

degradation, thereby inhibiting NF-κB activation. We cannot currently report on the mechanism by which HOXA1 interaction with RBCK1, or with TRAF2 regulates NF-κB signaling in our experiments. Possibly, HOXA1 regulates the TRAF2 ubiquitin ligase activity. Further conclusions await studies into the ubiquitin signaling that could be involved.

The NF-κB and HOXA1 interconnection is reinforced by their functional relationship with *miR-10a. HOXA1* has been reported as a direct downstream target of *mirR-10a.* During megakaryocytic differentiation, *miR-10a* is sharply down-regulated and *HOXA1* is correlatively upregulated (62). In the chronic pro-inflammatory state of arterial endothelial cells in atherosclerosis regions, local *miR-10a* expression is lowered whereas HOXA1 expression is upregulated (63). In human aortic endothelial cells, *miR-10a* inhibition causes HOXA1 upregulation both at the mRNA and protein levels. Strikingly, NF-κB-mediated inflammation was also identified as one of the most upregulated biological processes in *miR-10a* knockdown cells. Consistently, phosphorylation of IκB is significantly up-regulated upon *miR-10a* knockdown in human aortic endothelial cells, and this is accompanied by the increased nuclear localization of NF-κB p65 and expression of pro-inflammatory biomarkers like TNFα and interleukin-8 (IL-8) (63). This NF-κB, HOXA1 and *miR-10a* relationship is therefore supportive of a possible link between HOXA1 and megakaryocytopoiesis as well as inflammation.

The HOXA1 sequence shows an intriguing feature in two His repeats. Among homopolymeric tracts, His repeats are relatively rare (64) and it has been reported that only 86 human proteins contain stretches of five or more His residues (65). The physicochemical properties of His make it a versatile amino acid that can fulfill different roles, influencing protein conformation and enzymatic activity. Such His repeats can be found in Zn-finger domains that bind promoter DNA (66). Nevertheless, the function of these His repeats is underexplored. Variations in HOXA1 His repeat length have been reported in cases of autism in the Japanese population (18) and His deletion variants within the HOXA1 sequence have also been pointed to critically influence the function of the HOXA1 protein (20). Here we highlighted that the longer His repeat and the homeodomain of HOXA1 are crucial for establishing contacts with RBCK1 and TRAF2 and to activate NF-κB. We demonstrated that the HOXA1 mutants lacking the longest His repeat or the homeodomain are unable to activate NF-κB and to stimulate IL-8 secretion.

HOXA1 has been reported as a human mammary epithelial oncogene that modulates the STAT and the p44/42 MAP kinase pathways to promote cell survival, proliferation and relieves human mammary cells from contact inhibition *in vitro* (11,13,16,53). Among the hallmaks of cancer, we focused on the ability of cancer cells to lose contact inhibition that gives rise to focus formation (16,52) whereas cell-to-cell contacts formed by normal epithelial cells when they reach confluence operate to suppress further cell proliferation. As the ability to HOXA1 to trigger foci formation in MCF7 cells has been described previously (16), we here demonstrated that blocking the NF-κB pathway abolishes this foci formation related to HOXA1 expression. As

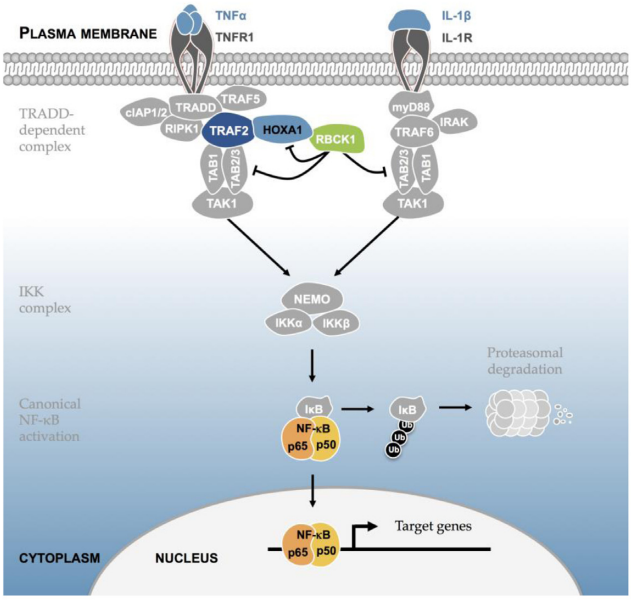

Figure 9. Model for the HOXA1-mediated modulation of the NF-κB pathway. Upon TNF stimulation, TNFα binding to TNFR initiates the recruitment of TRADD that further recruits cIAP1/2, RIPK1, TRAF2 and TRAF5 to form the TRADD-dependent complex. This leads to the docking of TAK1 in complex with TAB2 and TAB3, allowing formation of the IKK complex. The IKK complex phosphorylates IκB, promoting its proteasomal degradation, allowing NF-κB release and finally its nuclear translocation to engage transcriptional programs. On the one hand, HOXA1 enhances TRAF2 activity or stabilizes the TRADD-dependent complex to activate the TNF/NF-κB pathway. On the other hand, RBCK1 inhibits HOXA1 as well as TAB2/3 to repress NF-κB activation. In addition, RBCK1 and TRAF2 can compete with each other to bind either the 11-His repeat or the homeodomain of HOXA1 (not represented).

HOXA1 was also reported as increasing the proliferation rate of human breast cells (11,16), we hereby demonstrated that the inhibition of the NF-κB pathway prevents HOXA1 to enhance proliferation signaling, leading to oncogenic transformation (52). NF-κB activation is then crucial for HOXA1-mediated oncogenesis.

Together, our data are supportive of a model (Figure 9) in which HOXA1 interacts with TRAF2 to stabilize the TRADD-dependent complex and/or to enhance TRAF2 activity, triggering NF-κB activation. On the other hand, HOXA1 is inhibited by RBCK1 as RBCK1 expression represses HOXA1-induced NF-κB activation. HOXA1 could also inhibit RBCK1 ability to mediate TAB2/3 degradation since the inhibitory input RBCK1 exerts on NF-κB is partially relieved by HOXA1. Thus, HOXA1 and RBCK1 could display reciprocally inhibitory influences. Finally, HOXA1 proteins lacking the 11-His repeat or the homeodomain are unable to activate NF-κB because they cannot bind TRAF2 and cannot inhibit RBCK1. Correlatively, considering that RBCK1 and TRAF2 seem to bind the same determinants of HOXA1, they could compete each other for HOXA1 interaction.

While TNFα or IL-1β exposure can lead to NF-κB activation, it could also activate other signaling routes like the JNK, p38 MAPK, necrosis or apoptosis pathways that share the need of the TRADD-related platform for com-

plete activation (67). The ability of HOXA1 to interfere with those pathways remains to be further investigated, as well as the possible physical association between HOXA1 and the TRADD-dependent complex.

SUPPLEMENTARY DATA

Supplementary Data are available at NAR Online.

ACKNOWLEDGEMENTS

We thank Prof. Yves-Jacques Schneider (Université catholique de Louvain, Belgium) for the PGL4.32[luc2P/NF-κB-RE/Hygro] plasmid, Dr John Ashton (University of Rochester, New-York, USA) for the IκB-SR plasmid, Dr Tse-Hua Tan (National Health Research Institute, Zhunan, Taiwan) for the vectors coding for sh-TRAF2 and Prof. Deneen Wellik (University of Michigan, Ann Arbor, MI, USA) for the HOXA9, HOXB9 and HOXD9 plasmids. We thank Catherine Rasse (SMCS, Université Catholique de Louvain, Belgium) for the statistical analyses and Dr Jan Koster (Department of Oncogenomics, Academic Medical Center, Amsterdam, The Netherlands) for access to and advice on R2.

FUNDING

'Fonds de la Recherche Scientifique Médicale' from the Belgian National Fund for Scientific Research (FRS-FNRS) [3.4.536.06.F]; Belgian Foundation against Cancer; 'Fonds Spéciaux de Recherche' (UCL); FNRS research assistant grant (FRS-FNRS)(to A.D.); FRIA Fellowship (FRS-FNRS) (to B.L.). Funding for open access charge: Action de Recherche Concertée (ARC) [12./17.-.041].
Conflict of interest statement. None declared.

REFERENCES

1. Rezsohazy,R., Saurin,A.J., Maurel-Zaffran,C. and Graba,Y. (2015) Cellular and molecular insights into Hox protein action. *Development*, **142**, 1212–1227.
2. Alexander,T., Nolte,C. and Krumlauf,R. (2009) Hox genes and segmentation of the hindbrain and axial skeleton. *Annu. Rev. Cell Dev. Biol.*, **25**, 431–456.
3. Makki,N. and Capecchi,M.R. (2010) Hoxa1 lineage tracing indicates a direct role for Hoxa1 in the development of the inner ear, the heart, and the third rhombomere. *Dev. Biol.*, **341**, 499–509.
4. Chisaka,O., Musci,T.S. and Capecchi,M.R. (1992) Developmental defects of the ear, cranial nerves and hindbrain resulting from targeted disruption of the mouse homeobox gene Hox-1.6. *Nature*, **355**, 516–520.
5. Mark,M., Lufkin,T., Vonesch,J.L., Ruberte,E., Olivo,J.C., Dolle,P., Gorry,P., Lumsden,A. and Chambon,P. (1993) Two rhombomeres are altered in Hoxa-1 mutant mice. *Development*, **119**, 319–338.
6. Makki,N. and Capecchi,M.R. (2012) Cardiovascular defects in a mouse model of HOXA1 syndrome. *Hum. Mol. Genet.*, **21**, 26–31.
7. Abe,M., Hamada,J., Takahashi,O., Takahashi,Y., Tada,M., Miyamoto,M., Morikawa,T., Kondo,S. and Moriuchi,T. (2006) Disordered expression of HOX genes in human non-small cell lung cancer. *Oncol. Rep.*, **15**, 797–802.
8. Bitu,C.C., Destro,M.F., Carrera,M., da Silva,S.D., Graner,E., Kowalski,L.P., Soares,F.A. and Coletta,R.D. (2012) HOXA1 is overexpressed in oral squamous cell carcinomas and its expression is correlated with poor prognosis. *BMC Cancer*, **12**, 146.
9. Cantile,M., Pettinato,G., Procino,A., Feliciello,I., Cindolo,L. and Cillo,C. (2003) In vivo expression of the whole HOX gene network in human breast cancer. *Eur. J. Cancer*, **39**, 257–264.
10. Maeda,K., Hamada,J., Takahashi,Y., Tada,M., Yamamoto,Y., Sugihara,T. and Moriuchi,T. (2005) Altered expressions of HOX genes in human cutaneous malignant melanoma. *Int. J. Cancer*, **114**, 436–441.
11. Zhang,X., Zhu,T., Chen,Y., Mertani,H.C., Lee,K.O. and Lobie,P.E. (2003) Human growth hormone-regulated HOXA1 is a human mammary epithelial oncogene. *J. Biol. Chem.*, **278**, 7580–7590.
12. Wang,H., Liu,G., Shen,D., Ye,H., Huang,J., Jiao,L. and Sun,Y. (2015) HOXA1 enhances the cell proliferation, invasion and metastasis of prostate cancer cells. *Oncol. Rep.*, **34**, 1203–1210.
13. Mohankumar,K.M., Perry,J.K., Kannan,N., Kohno,K., Gluckman,P.D., Emerald,B.S. and Lobie,P.E. (2008) Transcriptional activation of signal transducer and activator of transcription (STAT) 3 and STAT5B partially mediate homeobox A1-stimulated oncogenic transformation of the immortalized human mammary epithelial cell. *Endocrinology*, **149**, 2219–2229.
14. Wolberger,C. (1996) Homeodomain interactions. *Curr. Opin. Struct. Biol.*, **6**, 62–68.
15. Remacle,S., Abbas,L., De Backer,O., Pacico,N., Gavalas,A., Gofflot,F., Picard,J.J. and Rezsohazy,R. (2004) Loss of function but no gain of function caused by amino acid substitutions in the hexapeptide of Hoxa1 in vivo. *Mol. Cell. Biol.*, **24**, 8567–8575.
16. Delval,S., Taminiau,A., Lamy,J., Lallemand,C., Gilles,C., Noel,A. and Rezsohazy,R. (2011) The Pbx interaction motif of Hoxa1 is essential for its oncogenic activity. *PLoS One*, **6**, e25247.
17. Hong,Y.S., Kim,S.Y., Bhattacharya,A., Pratt,D.R., Hong,W.K. and Tainsky,M.A. (1995) Structure and function of the HOX A1 human homeobox gene cDNA. *Gene*, **159**, 209–214.
18. Paraguison,R.C., Higaki,K., Sakamoto,Y., Hashimoto,O., Miyake,N., Matsumoto,H., Yamamoto,K., Sasaki,T., Kato,N. and Nanba,E. (2005) Polyhistidine tract expansions in HOXA1 result in intranuclear aggregation and increased cell death. *Biochem. Biophys. Res. Commun.*, **336**, 1033–1039.
19. Paraguison,R.C., Higaki,K., Yamamoto,K., Matsumoto,H., Sasaki,T., Kato,N. and Nanba,E. (2007) Enhanced autophagic cell death in expanded polyhistidine variants of HOXA1 reduces PBX1-coupled transcriptional activity and inhibits neuronal differentiation. *J. Neurosci. Res.*, **85**, 479–487.
20. Liu,J., Wang,B., Chen,X., Li,H., Wang,J., Cheng,L., Ma,X. and Gao,B. (2013) HOXA1 gene is not potentially related to ventricular septal defect in Chinese children. *Pediatr. Cardiol.*, **34**, 226–230.
21. Bondos,S.E., Tan,X.X. and Matthews,K.S. (2006) Physical and genetic interactions link hox function with diverse transcription factors and cell signaling proteins. *Mol. Cell Proteomics*, **5**, 824–834.
22. Lambert,B., Vandeputte,J., Remacle,S., Bergiers,I., Simonis,N., Twizere,J.C., Vidal,M. and Rezsohazy,R. (2012) Protein interactions of the transcription factor Hoxa1. *BMC Dev. Biol.*, **12**, 29.
23. Tokunaga,F., Nakagawa,T., Nakahara,M., Saeki,Y., Taniguchi,M., Sakata,S., Tanaka,K., Nakano,H. and Iwai,K. (2011) SHARPIN is a component of the NF-kappaB-activating linear ubiquitin chain assembly complex. *Nature*, **471**, 633–636.
24. Vanden Berghe,T., Linkermann,A., Jouan-Lanhouet,S., Walczak,H. and Vandenabeele,P. (2014) Regulated necrosis: the expanding network of non-apoptotic cell death pathways. *Nat. Rev. Mol. Cell Biol.*, **15**, 135–147.
25. Haas,T.L., Emmerich,C.H., Gerlach,B., Schmukle,A.C., Cordier,S.M., Rieser,E., Feltham,R., Vince,J., Warnken,U., Wenger,T. *et al.* (2009) Recruitment of the linear ubiquitin chain assembly complex stabilizes the TNF-R1 signaling complex and is required for TNF-mediated gene induction. *Mol. Cell*, **36**, 831–844.
26. Tian,Y., Zhang,Y., Zhong,B., Wang,Y.Y., Diao,F.C., Wang,R.P., Zhang,M., Chen,D.Y., Zhai,Z.H. and Shu,H.B. (2007) RBCK1 negatively regulates tumor necrosis factor- and interleukin-1-triggered NF-kappaB activation by targeting TAB2/3 for degradation. *J. Biol. Chem.*, **282**, 16776–16782.
27. Ghosh,S., May,M.J. and Kopp,E.B. (1998) NF-kappa B and Rel proteins: evolutionarily conserved mediators of immune responses. *Annu. Rev. Immunol.*, **16**, 225–260.
28. Baeuerle,P.A. and Baltimore,D. (1988) I kappa B: a specific inhibitor of the NF-kappa B transcription factor. *Science*, **242**, 540–546.
29. Perkins,N.D. (2007) Integrating cell-signalling pathways with NF-kappaB and IKK function. *Nat. Rev. Mol. Cell Biol.*, **8**, 49–62.
30. Oeckinghaus,A., Hayden,M.S. and Ghosh,S. (2011) Crosstalk in NF-kappaB signaling pathways. *Nat. Immunol.*, **12**, 695–708.

31. Naugler,W.E. and Karin,M. (2008) NF-kappaB and cancer-identifying targets and mechanisms. *Curr. Opin. Genet. Dev.*, **18**, 19–26.
32. Gupta,S.C., Kim,J.H., Prasad,S. and Aggarwal,B.B. (2010) Regulation of survival, proliferation, invasion, angiogenesis, and metastasis of tumor cells through modulation of inflammatory pathways by nutraceuticals. *Cancer Metastasis Rev.*, **29**, 405–434.
33. Gilmore,T.D. (2007) Multiple myeloma: lusting for NF-kappaB. *Cancer Cell*, **12**, 95–97.
34. Englaro,W., Bahadoran,P., Bertolotto,C., Busca,R., Derijard,B., Livolsi,A., Peyron,J.F., Ortonne,J.P. and Ballotti,R. (1999) Tumor necrosis factor alpha-mediated inhibition of melanogenesis is dependent on nuclear factor kappa B activation. *Oncogene*, **18**, 1553–1559.
35. Fouad,T.M., Kogawa,T., Reuben,J.M. and Ueno,N.T. (2014) The role of inflammation in inflammatory breast cancer. *Adv. Exp. Med. Biol.*, **816**, 53–73.
36. Gustafsson,N., Zhao,C., Gustafsson,J.A. and Dahlman-Wright,K. (2010) RBCK1 drives breast cancer cell proliferation by promoting transcription of estrogen receptor alpha and cyclin B1. *Cancer Res.*, **70**, 1265–1274.
37. Shen,R.R., Zhou,A.Y., Kim,E., O'Connell,J.T., Hagerstrand,D., Beroukhim,R. and Hahn,W.C. (2013) TRAF2 is an NF-kappaB-activating oncogene in epithelial cancers. *Oncogene*, **34**, 209–216.
38. Revet,I., Huizenga,G., Chan,A., Koster,J., Volckmann,R., van Sluis,P., Ora,I., Versteeg,R. and Geerts,D. (2008) The MSX1 homeobox transcription factor is a downstream target of PHOX2B and activates the Delta-Notch pathway in neuroblastoma. *Exp. Cell Res.*, **314**, 707–719.
39. Rao,N.A., McCalman,M.T., Moulos,P., Francoijs,K.J., Chatziioannou,A., Kolisis,F.N., Alexis,M.N., Mitsiou,D.J. and Stunnenberg,H.G. (2011) Coactivation of GR and NFKB alters the repertoire of their binding sites and target genes. *Genome Res.*, **21**, 1404–1416.
40. Chen,J. and Ruley,H.E. (1998) An enhancer element in the EphA2 (Eck) gene sufficient for rhombomere-specific expression is activated by HOXA1 and HOXB1 homeobox proteins. *J. Biol. Chem.*, **273**, 24670–24675.
41. Matis,C., Chomez,P., Picard,J. and Rezsohazy,R. (2001) Differential and opposed transcriptional effects of protein fusions containing the VP16 activation domain. *FEBS Lett.*, **499**, 92–96.
42. Bergiers,I., Bridoux,L., Nguyen,N., Twizere,J.C. and Rezsohazy,R. (2013) The homeodomain transcription factor Hoxa2 interacts with and promotes the proteasomal degradation of the E3 ubiquitin protein ligase RCHY1. *PLoS One*, **8**, e80387.
43. Remacle,S., Shaw-Jackson,C., Matis,C., Lampe,X., Picard,J. and Rezsohazy,R. (2002) Changing homeodomain residues 2 and 3 of Hoxa1 alters its activity in a cell-type and enhancer dependent manner. *Nucleic Acids Res.*, **30**, 2663–2668.
44. Goudet,G., Delhalle,S., Biemar,F., Martial,J.A. and Peers,B. (1999) Functional and cooperative interactions between the homeodomain PDX1, Pbx, and Prep1 factors on the somatostatin promoter. *J. Biol. Chem.*, **274**, 4067–4073.
45. Lambert,B., Vandeputte,J., Desmet,P.M., Hallet,B., Remacle,S. and Rezsohazy,R. (2010) Pentapeptide insertion mutagenesis of the Hoxa1 protein: mapping of transcription activation and DNA-binding regulatory domains. *J. Cell. Biochem.*, **110**, 484–496.
46. Yang,C.Y., Chiu,L.L. and Tan,T.H. (2016) TRAF2-mediated Lys63-linked ubiquitination of DUSP14/MKP6 is essential for its phosphatase activity. *Cell. Signal.*, **28**, 145–151.
47. Topisirovic,I., Guzman,M.L., McConnell,M.J., Licht,J.D., Culjkovic,B., Neering,S.J., Jordan,C.T. and Borden,K.L. (2003) Aberrant eukaryotic translation initiation factor 4E-dependent mRNA transport impedes hematopoietic differentiation and contributes to leukemogenesis. *Mol. Cell. Biol.*, **23**, 8992–9002.
48. Topisirovic,I., Kentsis,A., Perez,J.M., Guzman,M.L., Jordan,C.T. and Borden,K.L. (2005) Eukaryotic translation initiation factor 4E activity is modulated by HOXA9 at multiple levels. *Mol. Cell. Biol.*, **25**, 1100–1112.
49. Rothe,M., Wong,S.C., Henzel,W.J. and Goeddel,D.V. (1994) A novel family of putative signal transducers associated with the cytoplasmic domain of the 75 kDa tumor necrosis factor receptor. *Cell*, **78**, 681–692.
50. Rothe,M., Sarma,V., Dixit,V.M. and Goeddel,D.V. (1995) TRAF2-mediated activation of NF-kappa B by TNF receptor 2 and CD40. *Science*, **269**, 1424–1427.
51. Hsu,H., Shu,H.B., Pan,M.G. and Goeddel,D.V. (1996) TRADD-TRAF2 and TRADD-FADD interactions define two distinct TNF receptor 1 signal transduction pathways. *Cell*, **84**, 299–308.
52. Hanahan,D. and Weinberg,R.A. (2011) Hallmarks of cancer: the next generation. *Cell*, **144**, 646–674.
53. Mohankumar,K.M., Xu,X.Q., Zhu,T., Kannan,N., Miller,L.D., Liu,E.T., Gluckman,P.D., Sukumar,S., Emerald,B.S. and Lobie,P.E. (2007) HOXA1-stimulated oncogenicity is mediated by selective upregulation of components of the p44/42 MAP kinase pathway in human mammary carcinoma cells. *Oncogene*, **26**, 3998–4008.
54. Hanahan,D. and Weinberg,R.A. (2000) The hallmarks of cancer. *Cell*, **100**, 57–70.
55. Cogswell,P.C., Guttridge,D.C., Funkhouser,W.K. and Baldwin,A.S. Jr (2000) Selective activation of NF-kappa B subunits in human breast cancer: potential roles for NF-kappa B2/p52 and for Bcl-3. *Oncogene*, **19**, 1123–1131.
56. Wang,W., Nag,S.A. and Zhang,R. (2015) Targeting the NFkappaB signaling pathways for breast cancer prevention and therapy. *Curr. Med. Chem.*, **22**, 264–289.
57. Sovak,M.A., Bellas,R.E., Kim,D.W., Zanieski,G.J., Rogers,A.E., Traish,A.M. and Sonenshein,G.E. (1997) Aberrant nuclear factor-kappaB/Rel expression and the pathogenesis of breast cancer. *J. Clin. Ivestig.*, **100**, 2952–2960.
58. Nakshatri,H., Bhat-Nakshatri,P., Martin,D.A., Goulet,R.J. Jr and Sledge,G.W. Jr (1997) Constitutive activation of NF-kappaB during progression of breast cancer to hormone-independent growth. *Mol. Cell. Biol.*, **17**, 3629–3639.
59. Huber,M.A., Azoitei,N., Baumann,B., Grunert,S., Sommer,A., Pehamberger,H., Kraut,N., Beug,H. and Wirth,T. (2004) NF-kappaB is essential for epithelial-mesenchymal transition and metastasis in a model of breast cancer progression. *J. Clin. Invest.*, **114**, 569–581.
60. Liu,M., Sakamaki,T., Casimiro,M.C., Willmarth,N.E., Quong,A.A., Ju,X., Ojeifo,J., Jiao,X., Yeow,W.S., Katiyar,S. *et al.* (2010) The canonical NF-kappaB pathway governs mammary tumorigenesis in transgenic mice and tumor stem cell expansion. *Cancer Res.*, **70**, 10464–10473.
61. Chaturvedi,M.M., Sung,B., Yadav,V.R., Kannappan,R. and Aggarwal,B.B. (2011) NF-kappaB addiction and its role in cancer: 'one size does not fit all'. *Oncogene*, **30**, 1615–1630.
62. Garzon,R., Pichiorri,F., Palumbo,T., Iuliano,R., Cimmino,A., Aqeilan,R., Volinia,S., Bhatt,D., Alder,H., Marcucci,G. *et al.* (2006) MicroRNA fingerprints during human megakaryocytopoiesis. *Proc. Natl. Acad. Sci. U.S.A.*, **103**, 5078–5083.
63. Fang,Y., Shi,C., Manduchi,E., Civelek,M. and Davies,P.F. (2010) MicroRNA-10a regulation of proinflammatory phenotype in athero-susceptible endothelium in vivo and in vitro. *Proc. Natl. Acad. Sci. U.S.A.*, **107**, 13450–13455.
64. Faux,N.G., Bottomley,S.P., Lesk,A.M., Irving,J.A., Morrison,J.R., de la Banda,M.G. and Whisstock,J.C. (2005) Functional insights from the distribution and role of homopeptide repeat-containing proteins. *Genome Res.*, **15**, 537–551.
65. Salichs,E., Ledda,A., Mularoni,L., Alba,M.M. and de la Luna,S. (2009) Genome-wide analysis of histidine repeats reveals their role in the localization of human proteins to the nuclear speckles compartment. *PLoS Genet.*, **5**, e1000397.
66. Gamsjaeger,R., Liew,C.K., Loughlin,F.E., Crossley,M. and Mackay,J.P. (2007) Sticky fingers: zinc-fingers as protein-recognition motifs. *Trends Biochem.*, **32**, 63–70.
67. Aggarwal,B.B. (2003) Signalling pathways of the TNF superfamily: a double-edged sword. *Nat. Rev. Immunol.*, **3**, 745–756.